AD-A069 724 CALIFORNIA UNIV BERKELEY SPACE SCIENCES LAB F/G 4/1
A STUDY TO RELATE INTERPLANETARY MAGNETIC FIELD PARAMETERS TO A--ETC(U)
DEC 78 C MENG, K A ANDERSON F19628-76-C-0125
UNCLASSIFIED SERIES-20-ISSUE-1 AFGL-TR-79-0022 NL

| OF |
AD
A069 724

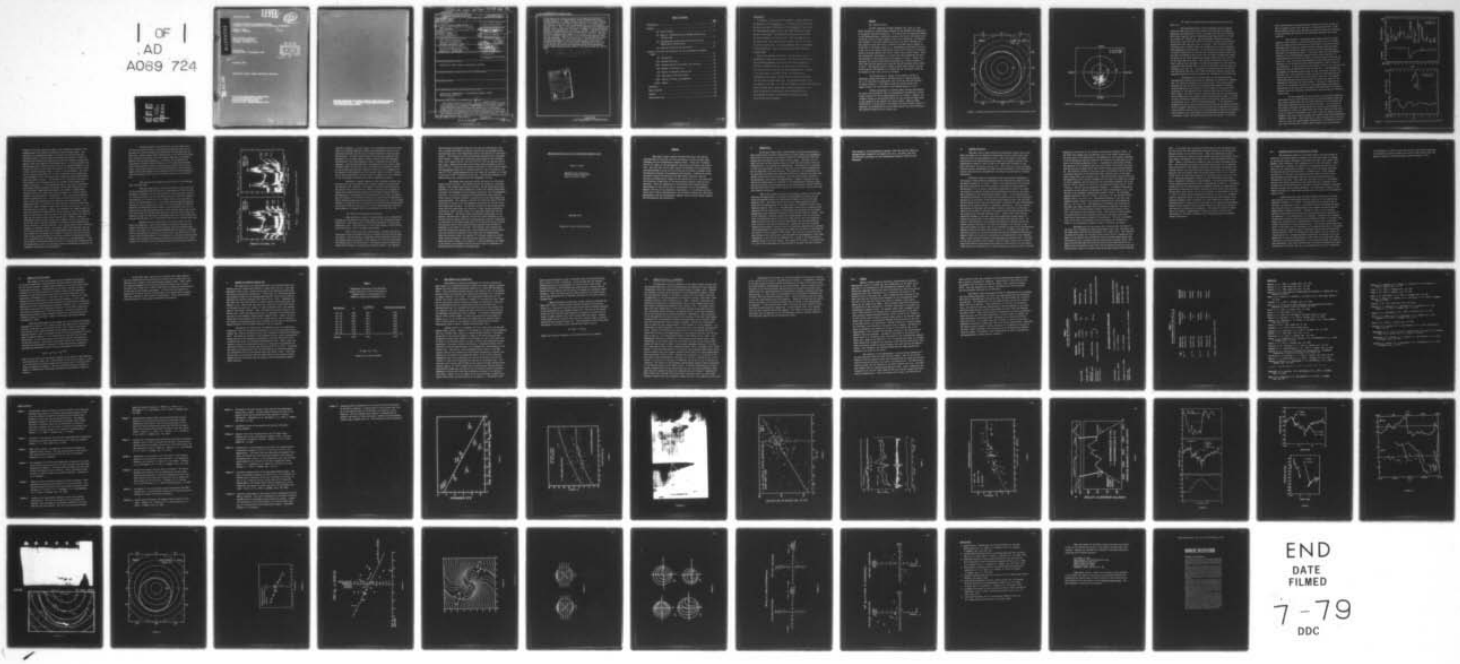

END
DATE
FILMED
7-79
DDC

LEVEL II

AFGL-TR-79-0022

# A STUDY TO RELATE INTERPLANETARY MAGNETIC FIELD PARAMETERS TO AURORAL PHENOMENA

Ching -I. Meng
Kinsey A. Anderson

Space Sciences Laboratory
University of California
Berkeley, California 94720



Final Report
15 March 1976 - 30 September 1978

December 1978



AIR FORCE GEOPHYSICS LABORATORY
AIR FORCE SYSTEMS COMMAND
UNITED STATES AIR FORCE
HANSCOM AFB, MASSACHUSETTS 01731

(9) Final rept. 15 Mar 76-30 Sep 78,

UNCLASSIFIED

SECURITY CLASSIFICATION OF THIS PAGE (When Data Entered)

| (19) REPORT DOCUMENTATION PAGE | | READ INSTRUCTIONS BEFORE COMPLETING FORM |
|---|---|---|
| 1. REPORT NUMBER (18) AFGL-TR-79-0022 | 2. GOVT ACCESSION NO. | 3. RECIPIENT'S CATALOG NUMBER |
| 4. TITLE (and Subtitle) (6) A Study to Relate Interplanetary Magnetic Field Parameters to Auroral Oval Phenomena, | | 5. TYPE OF REPORT & PERIOD COVERED Final 3/15/76-9/30/78 |
| | | 6. PERFORMING ORG. REPORT NUMBER (14) Series-20, Issue-1 |
| 7. AUTHOR(s) (10) Ching -I. Meng, Kinsey A. Anderson | | 8. CONTRACT OR GRANT NUMBER(s) (15) F19628-76-C-0125 new |
| 9. PERFORMING ORGANIZATION NAME AND ADDRESS Space Sciences Laboratory, University of California, Berkeley, California 94720 | | 10. PROGRAM ELEMENT, PROJECT, TASK AREA & WORK UNIT NUMBERS 62101F (16) 7663 (17) 08 |
| 11. CONTROLLING OFFICE NAME AND ADDRESS Air Force Geophysics Laboratory, Hanscom AFB, Massachusetts 01731, Monitor/B. S. Dandeker/PHI | | 12. REPORT DATE (11) Dec 78 |
| | | 13. NUMBER OF PAGES (12) 65p. |
| 14. MONITORING AGENCY NAME & ADDRESS (if different from Controlling Office) | | 15. SECURITY CLASS. (of this report) Unclassified |
| | | 15a. DECLASSIFICATION/DOWNGRADING SCHEDULE |

16. DISTRIBUTION STATEMENT (of this Report)

Approved for public release; distribution unlimited

17. DISTRIBUTION STATEMENT (of the abstract entered in Block 20, if different from Report)

18. SUPPLEMENTARY NOTES

19. KEY WORDS (Continue on reverse side if necessary and identify by block number)

Auroral oval, Magnetosphere, Interplanetary Magnetic Field, Magnetospheric Substorm

(of a)

20. ABSTRACT (Continue on reverse side if necessary and identify by block number)

This report consists of two parts. The first part summarizes the major results (of this report) on the study of auroral oval phenomena and interplanetary magnetic field, supported by this contract. These results can be grouped under 8 categories and reported in 8 scientific papers which are published or already accepted for publication by referred international journals. The second part presents an up-dated understanding on the auroral oval phenomena and their relation with the interplanetary magnetic field.

(over)

DD FORM 1 JAN 73 1473 EDITION OF 1 NOV 65 IS OBSOLETE

UNCLASSIFIED

SECURITY CLASSIFICATION OF THIS PAGE (When Data Entered)

328950

(cont)

It was based on an invited talk given at the American Geophysical Union Chapman Conference on "Magnetospheric Substorms and Related Plasma Processes" ~~held~~ at Los Alamos, October 9-13, 1978. It reviews research involved with direct and inferred determinations of the polar cap size and location, as well as their relationships with the interplanetary magnetic field. First, the progress in the observation and understanding of polar cap size variations as related to changes of the interplanetary magnetic field magnitude and direction is reported. Obtained by scaling the global auroral distributions from DMSP auroral pictures, some new results on configurational changes of the auroral oval (i.e., the polar cap) with different orientations of the interplanetary magnetic field are also discussed. There are indications of the dawn-dusk and sunward-tailward displacements of the auroral oval in association with the interplanetary magnetic field $B_y$ and $B_x$ components, respectively. It is obvious from this review that a better understanding of the interaction between the terrestrial magnetosphere and the interplanetary magnetic field requires further efforts, both observational and theoretical.

X

B sub y and B sub x

## TABLE OF CONTENTS

## INTRODUCTION

The behavior of high latitude ionosphere is closely related to the morphology of the auroral oval. The auroral oval encircles the the polar cap, which is the region of open geomagnetic field lines. The interplanetary magnetic field (IMF) lines would have an easy access to this region. The merging processes would also control the size and shape of the auroral oval. Thus the morphology of the auroral oval has to deal with the study of the IMF, the polar cap and the auroral oval. The study presented here is based mainly on the observations from the Defense Meteorological Satellite Program (DMSP).

Some of the important results are: (a) The auroral oval is mathematically represented by a circle with its center offset from the corrected geomagnetic (CG) pole and the radius dependent on the level of magnetic activity. (b) The flux of soft electrons over the north and south polar caps shows asymmetry and is related to the orientation of the IMF. (c) The low energy electron precipitation of the polar cap electrons show opposite gradients over the north and south polar caps. The gradients depends on the $B_y$ component of the IMF. (d) The direct dumping of plasma sheet electrons, produce diffuse aurora, whereas the electrons responsible for the polar cap aurora are plasma sheet electrons passing through the acceleration region located between the equatorial plasma sheet and the polar atmosphere.

## RESULTS

### (1) Auroral Circle

In 1975, *Holzworth and Meng (Geophys. Res. Lett., p. 377, 1975)* introduced a curve-fitting technique for the mathematical expression of the global auroral distribution. It is found that the poleward boundary of the Feldstein-Starkov statistical auroral oval can be represented by an off-center circle in dipole magnetic local time coordinates. By applying this analysis to the quiet bright auroral arc (or arcs) extending over many magnetic local time hours, recorded by the DMSP auroral images, we found that an off-center circle (i.e., the simplest second-order curve) is a best fit to the auroral distribution within $\pm$ 0.5° accuracy in latitude. Several different methods were used to verify this circular nature. Thus, the instantaneous distribution of auroral arcs which delineate the poleward boundary of the auroral oval has a shape of a circle. Figure 1 illustrates the auroral distribution represented by a circle centered at 3.93° away from the dipole pole along the 2230 MLT meridian with a radius of 18.6°. The observed aurora is shown by small open circles, the difference between the observed arc location and the calculated circle has an average of only 0.20° $\pm$ 0.15° in latitude.

The distribution of centers of the auroral circles is generally concentrated within a circular area of 3° radius centered at $\sim$ 4.2° away from the geomagnetic pole toward the 0015 MLT meridian as shown in Figure 2. The radius of auroral circles varies over a range of about $\pm$ 5° with respect to the average radius of $\sim$ 19°.

Without photographs of complete global auroral distribution we cannot prove definitely that the instantaneous distribution of quiet bright auroral arcs can be approximated well by a circle. However, the circular fitting to the observed auroral arc can provide an upper limit to the skewness of the auroral oval from a circle. Based on these observations, it may be proper to introduce the term 'auroral circle' to represent the distribution of quiet bright auroral arcs which delineate the poleward boundary of the auroral oval.

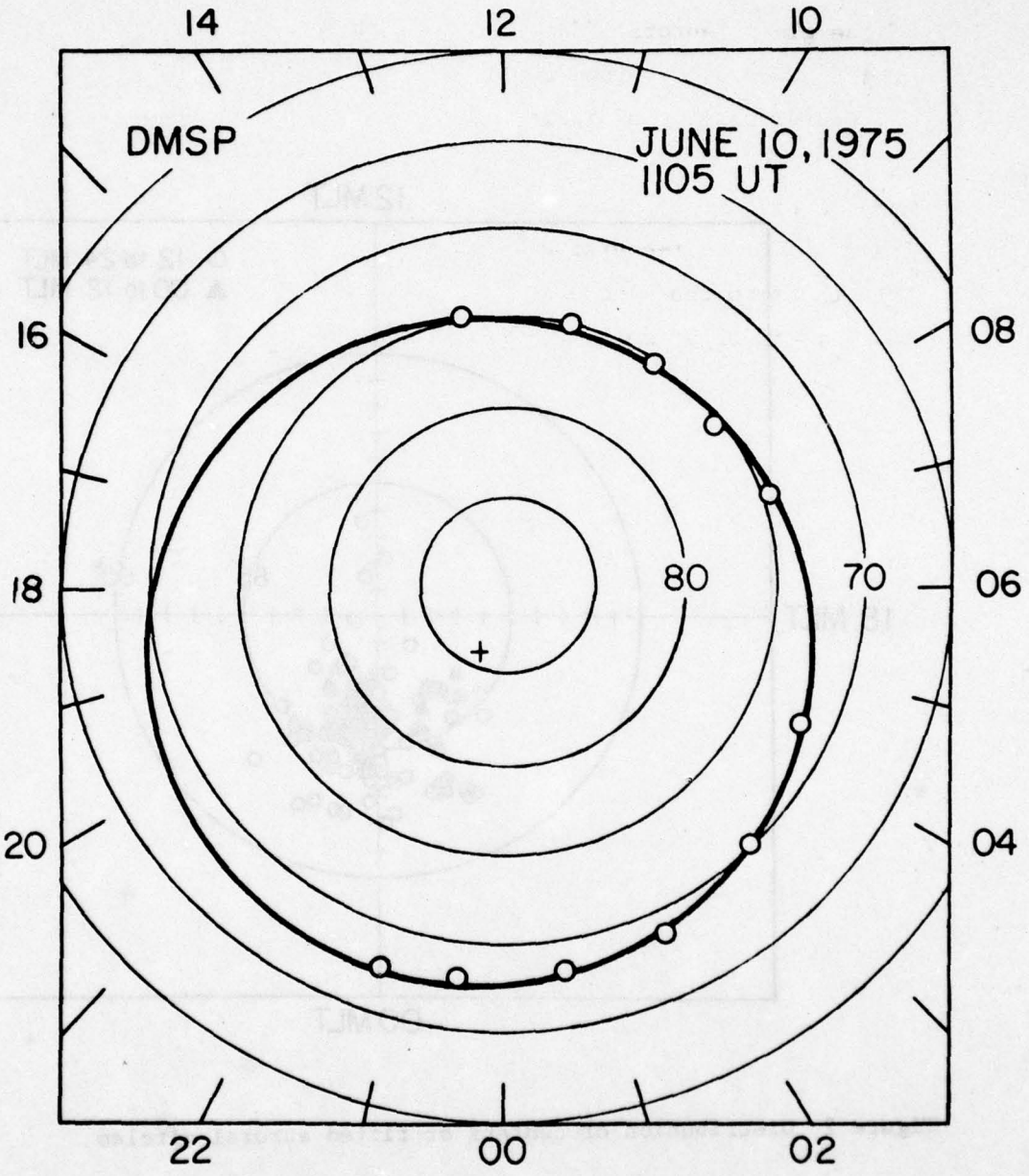


**Figure 1** Observed morning auroral distribution and the fitted auroral circle

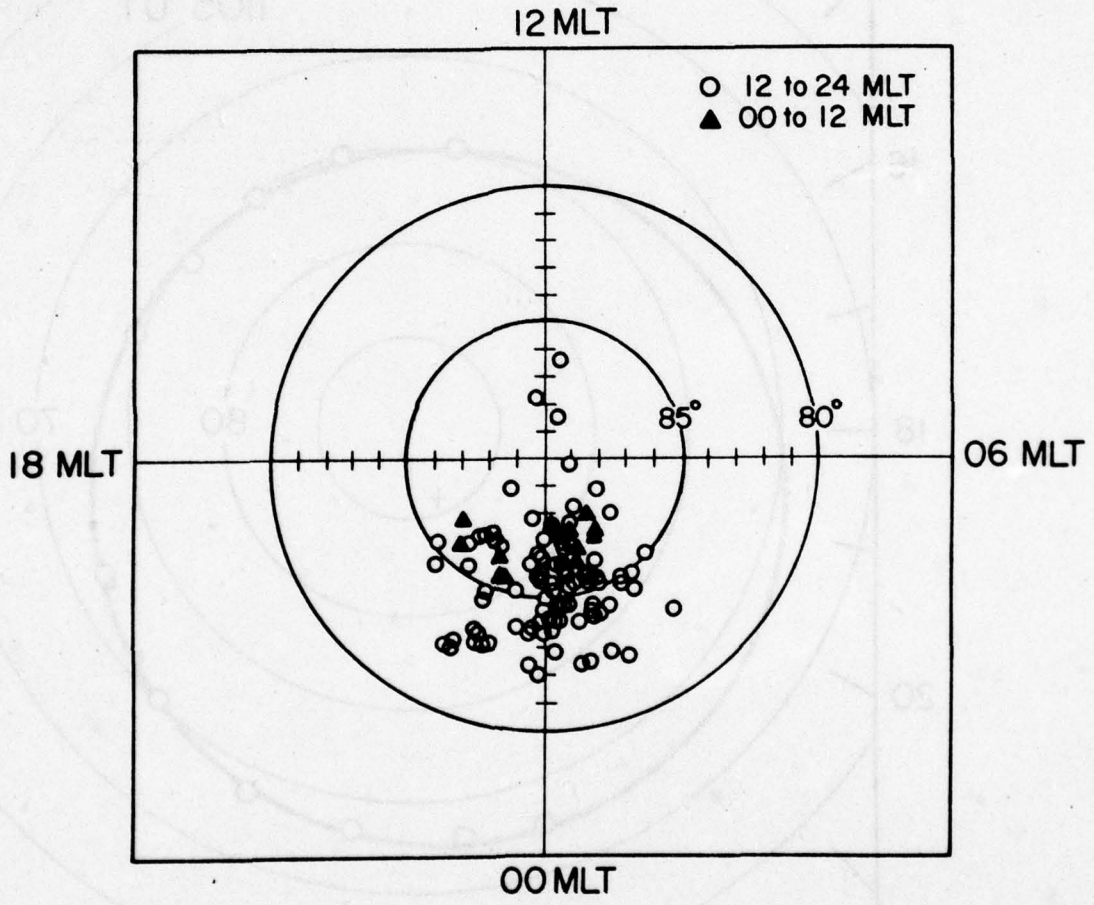


**Figure 2 Distribution of centers of fitted auroral circles**

(2) Entry of interplanetary low energy electrons over the polar cap.

The observations made by the low-energy electron detector aboard the DMSP 32 satellite have revealed that the polar cap regions sometimes were bombarded by intense low-energy electron fluxes, between 200 eV and a few keV, with an integrated energy flux (200 eV to 20 keV) up to about $10^{-1}$ erg/cm$^2$s sr. The precipitation differential flux at 200 eV can be more than $10^8$ el/cm$^2$s sr keV with a rather uniform spatial distribution over the entire polar cap region. The occurrence of this particular type of intense polar cap precipitation is closely associated with geomagnetic storm activity. It is also noticed that the intensity of electron fluxes was not the same over northern and southern polar caps and that the difference can be more than two orders of magnitude; namely, one polar cap was fully bombarded by intense fluxes while the other was at the quiet time noise level. The spectra of these electrons do not have a typical form; sometimes it can be approximated by a power law with a spectral index between about -1.5 and -3, and other times the power law assumption is a poor one. In general, the observed spectra are similar over the entire polar cap, even though distinctly different spectra were sometimes detected over the morningside and eveningside of the polar cap.

The observation of intense polar cap low-energy electron precipitation confirms the finding by *Winningham and Heikkila (J. Geophys. Res., 79, 1974)* who referred to it as polar rain. The uniform spatial distribution over the polar cap and the observed asymmetric northern-southern hemispheric distribution are very similar to the spatial characteristics of the energetic solar electron events detected over the polar region. The lower fluxes are soft electron polar cap precipitations and the magnetotail lobe observed during relatively quiet times are found to have a north-south asymmetry and also to be closely associated with the interplanetary (i.e., solar) low-energy electrons. It is important to determine the source of the observed intense polar cap low-energy electrons. We have compared variations of the 200 eV flux with variations of the solar flare energetic electron fluxes in the interplanetary space and the magnetotail observed by the Johns Hopkins University Applied Physics Laboratory experiments on IMP-7 and IMP-8 during the same time period. No relation

can be found between low-energy electron fluxes of the polar cap and the flux of energetic solar flare electrons in interplanetary space. Thus, the low-energy electrons over the polar cap reported cannot be attributed to the low-energy tail portion of the well-known energetic solar flare electrons.

The intensity of low-energy solar electron fluxes in interplanetary space is known to vary with solar activity; thus, the intense polar cap precipitation detected may be attributed to the entry of these low-energy solar electrons, and the intensity variation from the quiet time values may reflect the temporal variation of the low-energy solar electrons in interplanetary space. It has been shown that the azimuthal direction of the interplanetary magnetic field controls the entry of interplanetary particles into the north or south magnetotail lobe and the polar cap. Since the actual IMF measurements during this period are not available to us, we have shown the inferred polarity of IMF in Figures 3 for comparison. It can be seen that the intense northern polar cap events were associated with the IMF direction away from the sun. This relationship strengthens the suggested solar origin of these low-energy electrons over the polar cap. The occurrence of polar cap intense low-energy electron events may result from the solar wind electron variation. The apparent relationship between storms and the polar cap events may merely be two independent consequences of solar activity. In order to understand the entry of the low-energy electrons into the magnetosphere, simultaneous measurements in the polar cap, the high-latitude magnetotail, and interplanetary space are necessary; unfortunately, these data are not available at this time.

On the eveningside of the polar cap, a gap without significant low-energy electron fluxes between the polar cap precipitation region and the auroral precipitation belt was always observed, but its location and width change significantly from one orbit to another. If the source of the intense low-energy electron fluxes over the polar cap is indeed of interplanetary origin, the region where the intense fluxes of these electrons was observed corresponds to the "open" field line region; the geomagnetic field lines from this region are connected with the interplanetary magnetic field lines. Thus, these solar origin electrons can be used as a tracer to study the magnetospheric configuration. The existence of this gap, which was also seen in ISIS-1 data indicates that the equatorward

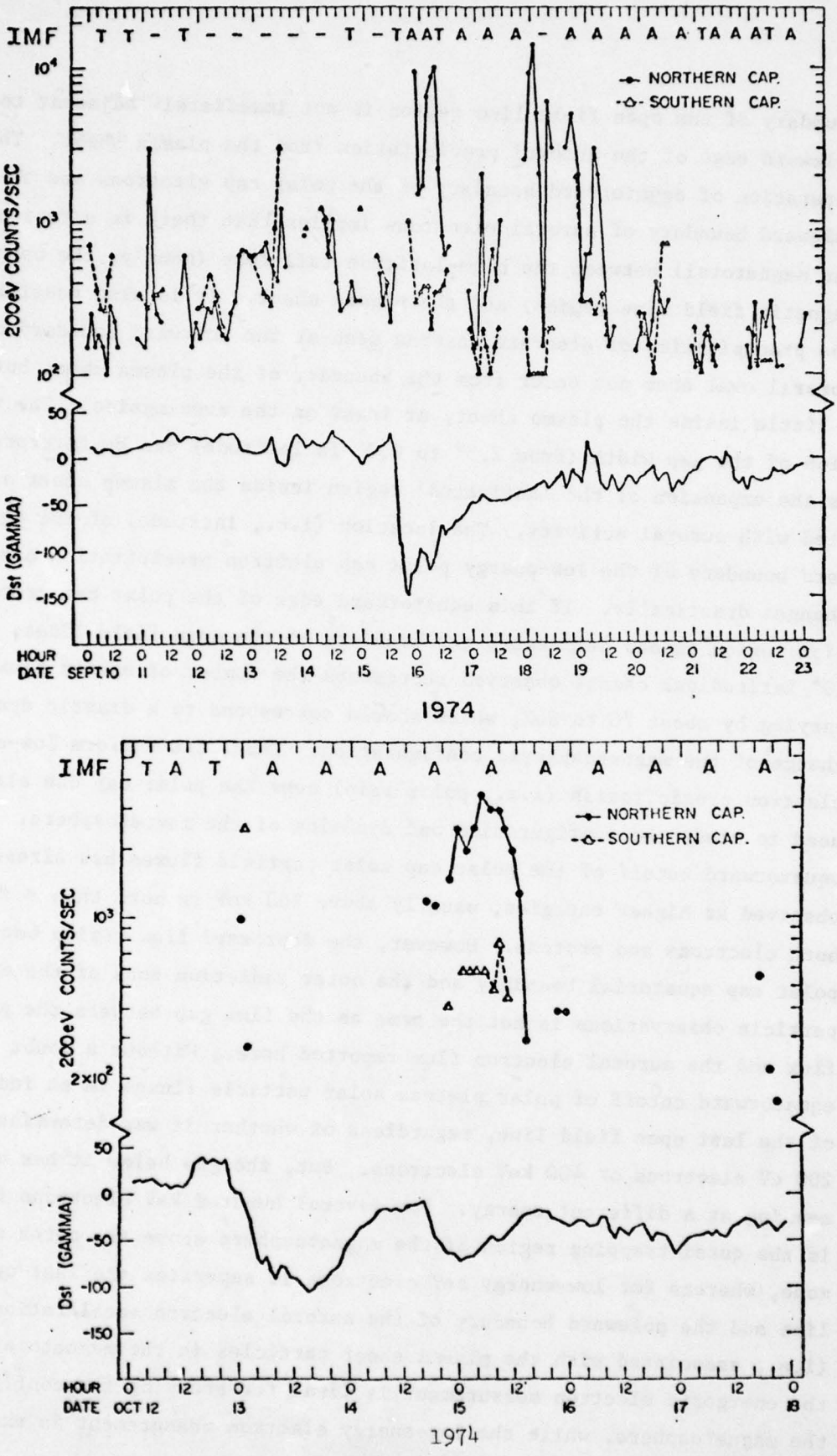


Figure 3 Variation of the polar cap fluxes and the orientation of the IMF.

boundary of the open field line region is not immediately adjacent to the poleward edge of the auroral precipitation from the plasma sheet. The separation of equatorward boundary of the polar cap electrons and the poleward boundary of auroral electrons implies that there is a region in the magnetotail between the high-latitude tail lobe (namely, the open geomagnetic field line region) and the plasma sheet. It is also possible that the precipitation of discrete auroras seen at the poleward boundary of the auroral oval does not occur from the boundary of the plasma sheet but from a little inside the plasma sheet, at least on the eveningside. The variation of the gap width (from 2.5° to 0.2° in latitude) can be interpreted as the expansion of the 'activated' region inside the plasma sheet associated with auroral activity. The location (i.e., latitude) of the equatorward boundary of the low-energy polar cap electron precipitation also changes drastically. If this equatorward edge of the polar cap precipitation region indeed delineates the boundary of the open field lines, the 10° latitudinal change observed represents the number of opened fluxes varying by about 70 to 80%, which should correspond to a drastic dynamic change of the magnetospheric configuration. Thus, the uniform low-energy electron precipitation (i.e., polar rain) over the polar cap can also be used to study the configuration and dynamics of the magnetosphere. The equatorward cutoff of the polar cap solar particle fluxes has already been observed at higher energies, usually above 100 keV to more than a few MeV, for both electrons and protons. However, the depressed flux region between the polar cap equatorial boundary and the outer radiation zone of the energetic particle observations is not the same as the flux gap between the polar cap flux and the auroral electron flux reported here. Without a doubt the equatorward cutoff of polar plateau solar particle fluxes is an indication of the last open field line, regardless of whether it was determined from 200 eV electrons or 400 keV electrons. But, the gap below it has a different meaning at a different energy. For several hundred keV electrons this gap is the quasi-trapping region of the magnetosphere above the outer electron zone, whereas for low-energy keV electrons it separates the last open field line and the poleward boundary of the auroral electron acceleration region (i.e., associated with the plasma sheet particles in the magnetotail). Thus, the energetic electron measurement is ideal for studying the configuration of the magnetosphere, while the low-energy electron measurement is excellent for examining the dynamics of the magnetotail.

The distribution of low-energy flux over the polar cap is not exactly uniform; usually a statistically meaningful difference in intensity was observed between the morningside and eveningside of the polar cap. During intense events examined here, over the northern polar cap, the fluxes were higher over the dawnside than over the duskside. Whether this dawn-dusk asymmetry of the fluxes can be explained by the asymmetric electric field configuration in an open magnetospheric model associated with different interplanetary magnetic field orientations, is not clear because of the lack of simultaneous interplanetary magnetic field information and the physical processes between asymmetric polar cap electric fields and the low-energy electrons over the polar cap.

(3) Interplanetary Magnetic Field Effect on the Low-Energy Solar Electron Entry

The low-energy electron observations made over the polar cap by the polar-orbiting DMSP 32 satellite at approximately 840-km altitude revealed an asymmetric intensity distribtuion of the low-energy electron (< 1 keV) precipitation in the dawn-dusk direction as shown in Figure 4. The direction of the gradient in the northern polar cap is opposite to that of the southern polar cap. It is found that the gradient direction depends on the $B_y$ component of the IMF. For a positive IMF $B_y$ value the intensity of the precipitation decreases from the morning sector to the evening sector over the northern polar cap and from the dusk sector to the dawn sector over the southern polar cap; for a negative IMF $B_y$ value the decrease is from the dusk sector to the dawn sector over the northern polar cap and from the dawn sector to the dusk sector over the southern polar cap.

Recent satellite observations cited earlier show that the polar cap regions are constantly bombarded by low-energy electrons and suggest that they are interplanetary electrons which have gained direct access to the polar cap. The present analysis reveals that these electrons are not precipitated uniformly over the polar cap, even though they do have a rather smooth distribution. If the electrons are indeed of interplanetary origin, this asymmetric precipitation indicates a nonuniform entry and/or transport of particles in the dawn-dusk direction with processes related to

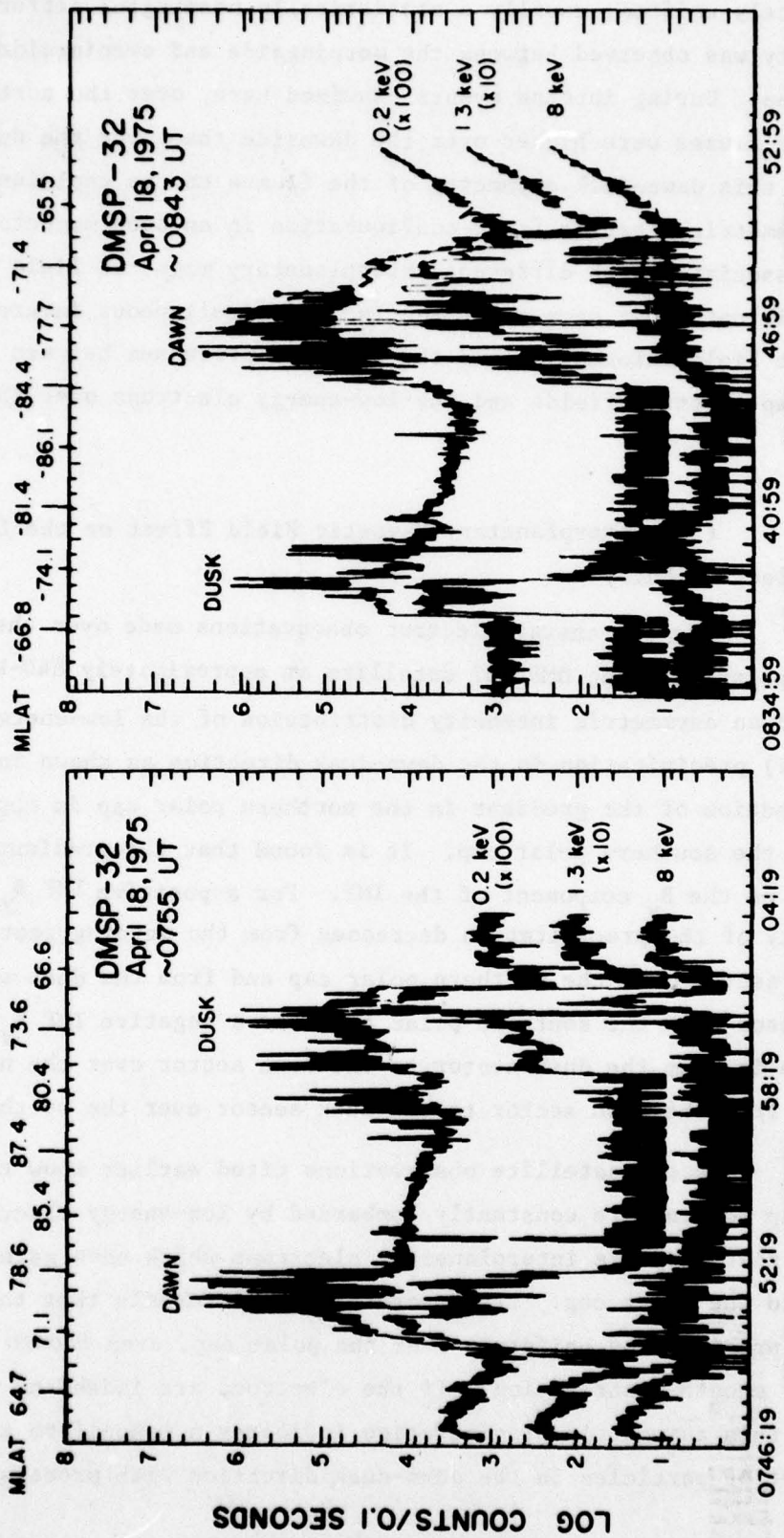


Figure 4. Gradient of the polar cap soft electrons observed at both hemispheres.

the IMF $B_y$ component. In this respect it is interesting to point out that there is a striking similarity between the precipitation pattern of the low-energy electrons and the electric field distribution along the dawn-dusk meridian. The OGO-6 electric field (the dawn-dusk component) measurements over the polar region revealed a similar dawn-dusk asymmetric distribution of the field magnitude, which is controlled by the IMF $B_y$ component. The dawn-dusk gradient of the magnitude of the electric field reversed between the two polar caps, and there is a correlation, similar to the electron precipitation, between the direction of the gradient of the electric field magnitude and the azimuthal angle of the IMF. Further, in the distant magnetotail at lunar orbit, an asymmetry of the occurrence of the lobe plasma controlled by the IMF $B_y$ component was found.

Therefore, a higher intensity of the low-energy electron flux over the polar cap is associated with a faster convection velocity from the dayside to the nightside. The pattern of the dawn-dusk gradient of the electron flux varies from one crossing to another, but in general it always has a simple monotonic change, as illustrated examples indicate. The magnitude of this gradient also changes from time to time; the difference in intensity of the electron flux can be from 1 order of magnitude to almost nothing between dawn and dusk edges of the polar cap. It is of great interest to compare the polar cap electron flux with the simultaneous polar cap electric field and convection for a better understanding of this dawn-dusk asymmetric low-energy electron precipitation over the polar cap.

(4) Electron Precipitations and Auroras

Many significant results of auroral physics were obtained from studying the simultaneous DMSP auroral images and the low-energy electron observation. Four papers on this subject are published or in press (see publication list). The following is a very brief summary of these results and details can be found in original publications.

Polar auroras have two distinct forms. Discrete auroras are distributed along the poleward half of the auroral oval and over the polar cap regions. Diffuse auroras, a widespread smooth luminosity, constitute the optical emission background of the auroral oval and also extend along the morning side of the auroral zone. Two distinct auroral electron precipitations correspond to the above two forms of auroras. The spatially

narrow-intense precipitation bands with the spectral peak between a few keV to several keV produce the discrete auroras and the extended uniform precipitations with a near Maxwellian spectral distribution for the diffuse auroras. The intensity of these precipitations increases with the geomagnetic activity. During quiet conditions, the discrete auroral electrons have a total energy flux of a few erg $cm^{-2}s^{-1}sr^{-1}$ and the spectral peak is near 3 keV. During active times, their energy fluxes increase to tens of erg $cm^{-2}s^{-1}sr^{-1}$ or more and the spectral peak moves to near 10 keV or higher. The precipitated energy flux of diffuse auroras is only a fraction of one erg $cm^{-2}s^{-1}sr^{-1}$ during geomagnetically quiet times and increases to at least a few erg $cm^{-2}s^{-1}sr^{-1}$ during the active time. The spectral hardness of the diffuse aurora also correlates with the geomagnetic activity.

The plasma sheet electrons provide the source for the precipitated auroral electrons. The diffuse auroras are produced by the direct dumping of the trapped plasma sheet electrons, and the strong pitch angle diffusion is the most likely mechanism to scatter the trapped plasma sheet electrons, and sometimes also the energetic electrons, into the atmospheric loss cone. The cyclotron resonance with electrostatic waves above the local electron cycletron frequency is believed to be the pitch angle scattering mechanism. The frequently observed soft equatorial edge of the diffuse aurora is likely to be the atmospheric projection of the soft earthward plasma sheet boundary. The discrete auroras are also caused by electrons from the plasma sheet, but they have to pass through the particle acceleration region located between the equatorial plasma sheet and the polar atmosphere. The recent rocket and satellite observations of the particle characteristics, magnetic and electric field variations in the discrete auroral region reveal that intense parallel electric fields exist at relatively low altitudes within about $10^4$ km above the Earth's surface. The potential drop of this upward pointing parallel electric field is generally in the range of a few keV. This electric field produces the observed monoenergetic spectral peak in the differential electron spectra and also accelerates ionospheric ions upward into the magnetosphere. Below this potential drop, the inverted 'V' structure appears and a discrete aurora is observed. How this parallel electric field is created above the auroral region is not clear yet. Plasma diagnostics are needed in the region of the parallel electric field in order to understand the physical processes involved in its generation.

# POLAR CAP VARIATIONS AND THE INTERPLANETARY MAGNETIC FIELD

Ching -I. Meng

Applied Physics Laboratory
The Johns Hopkins University
Laurel, Maryland 20810

DECEMBER 1978

Submitted to Space Science Reviews

## ABSTRACT

This paper reviews research involved with direct and inferred determinations of the polar cap size and location, as well as their relationships with the interplanetary magnetic field. "Polar cap" is defined here as the region of open geomagnetic field lines encircled by the auroral oval. The first part of the paper reports the progress in the observation and understanding of polar cap size variations as related to changes of the interplanetary magnetic field magnitude and direction. Obtained by scaling the global auroral distributions from DMSP auroral pictures, some new results on configurational changes of the auroral oval (i.e., the polar cap) with different orientations of the interplanetary magnetic field are also discussed. There are indications of the dawn-dusk and sunward-tailward displacements of the auroral oval in association with the interplanetary magnetic field $B_y$ and $B_x$ components, respectively. It is obvious from this review that a better understanding of the interaction between the terrestrial magnetosphere and the interplanetary magnetic field requires further efforts, both observational and theoretical.

## I. INTRODUCTION

In the past twenty years, various types of satellite observations have revealed that the earth's magnetosphere is open: namely that geomagnetic field lines from the polar cap regions extend into interplanetary space and connect with the magnetic field lines of solar origin. Variations of the solar wind and the interplanetary magnetic field will undoubtedly affect the configuration of the terrestrial magnetosphere. Associated with an increase of the solar wind dynamic pressure, compression of the dayside magnetosphere and the magnetotail has been detected. The location of the magnetopause can be accurately determined from magnetohydrodynamics by balancing the solar wind dynamic pressure in the interplanetary space with the magnetic pressure of the geomagnetic field inside the magnetosphere. However, responses of the terrestrial magnetosphere to variations of the interplanetary magnetic field are far from clear, and the importance of the interplanetary magnetic field in the solar-terrestrial interaction, especially in the energy coupling, has been just recently recognized.

One of the possible processes of the energy transfer from the solar wind into the magnetosphere to produce the magnetospheric substorm is the field line merging between the interplanetary magnetic field and the geomagnetic field. The dayside northward directed closed geomagnetic field lines near the magnetopause can be eroded away by a southward directed interplanetary magnetic field (i.e., the geomagnetic field lines are opened by and connected with the interplanetary field lines); and consequently the dayside magnetopause moves earthward (see *Russell, 1979* in this issue for review). Due to the "frozen-in" condition between the interplanetary field and the solar wind, the antisunward motion of the solar wind carries the newly merged geomagnetic field lines from the dayside magnetosphere (or the magnetosheath) across the polar cap into the magnetotail. Associated with this so-called "magnetic flux transfer" process, one of the expected configurational responses of the magnetosphere is the change in the polar cap size which is controlled by the number of open geomagnetic field lines. The polar cap is defined as the area bounded by the auroral oval, and the bundle of the geomagnetic field lines originating in the polar cap is connected (i.e., open) to the interplanetary magnetic field of the solar origin. The purpose of this paper is to report the progress in the observation and understanding of the polar cap size variation

with changes of the interplanetary magnetic field and some new results on configurational changes of the auroral oval (i.e., the polar cap) with the different orientation of the interplanetary magnetic field are also discussed.

## II. DAYSIDE VARIATIONS

The polar cusp at high altitude and the dayside auroral oval in the polar ionosphere are the boundaries delineating the last closed field lines from the region of open geomagnetic lines. Thus, the effect of the earthward motion of the dayside magnetopause during the southward turning of the interplanetary magnetic field is seen as the equatorward movements of the polar cusp and of the dayside auroral oval. Their locations can be determined from the particle measurements of polar orbiting satellites or from the optical auroral observations and ionosonde data by using the ground-based or airborne instruments.

The first report of the possible polar cusp motions responding to the changes of the north-south component of the interplanetary magnetic field was made by *Russell et al. (1971)*. Based on the characteristics of particles and fields observed by the OGO-5 satellite in the dayside magnetosphere at mid-altitude ($\sim$ 2.6 to 6 $R_e$), these authors identified the polar cusp region and compared its spatial location with simultaneous variations of the north-south component of the interplanetary magnetic field. It was concluded that the multiple detection of the identified cusp region along the OGO-5 trajectory appeared to be the effect of the interplanetary magnetic field, and also that the mid-altitude polar cusp moved equatorward or poleward when the interplanetary magnetic field turned southward or northward, respectively. The most convincing evidence of the polar cusp movements, however, comes from a statistical study of the location of the polar cusp electron precipitation measured by the low altitude polar orbiting satellite, OGO-4. *Burch (1972)* found that the equatorial boundary of the polar cusp moves equatorward several degrees in latitude during periods of the southward interplanetary magnetic field. In Figure 1, the ordinate $\Delta\Lambda$ is the difference between the observed and the expected invariant latitudes of the polar cusp boundary; the abscissa is the time delay between the sharp onset of the southward turning of the interplanetary magnetic field and the polar cusp observation. It is evident here that the equatorward motion of the polar cusp occurs during the southward interplanetary magnetic field and the polar cusp location is at progressively lower latitudes after a sharp southward turning of the interplanetary magnetic field. The slope of the linear regression line fitted to the data points reveals that the polar cusp moves gradually equatorward with a speed of approximately 0.1° per minute. These results are interpreted as a direct evidence for gradual erosion of dayside

geomagnetic field lines by the southward interplanetary magnetic field. As the field line merging plays an important role in the energy transfer from the solar wind to the magnetosphere, the magnitude of the southward component of the interplanetary magnetic field may be related to the efficiency of erosion of the dayside geomagnetic field. A quantitative relationship between the magnitude of the southward field and the latitude of the polar cusp location was observed by *Burch (1973)* from 54 OGO-4 polar cusp crossings (Figure 2). The invariant latitude of the polar cusp is the ordinate and the 45 minute-average magnitude of the north-south ($B_z$) component prior to the polar cusp crossing forms the horizontal axis. Both the poleward (open circles) and the equatorward (solid circles) boundaries of the polar cusp region are related to the $B_z$ component, and the curves are the least-square quadratic fit to the data ($\Lambda = 80.3^\circ + 0.76\ B_z - 0.03\ B_z^2$ for the poleward boundary and $\Lambda = 75.5^\circ + 0.53\ B_z - 0.05\ B_z^2$ for the equatorial boundary). A systematic lowering of the polar cusp was observed in conjunction with the decreasing $B_z$ (i.e., the increase of the southward interplanetary magnetic field). The equatorial boundary shifted by almost $5^\circ$ from $B_z = 0\gamma$ to $B_z = -6\gamma$ but only by $0.5^\circ$ for changes from $B_z = 6\gamma$ to $B_z = 2\gamma$. The poleward boundary of the polar cusp responded almost linearly to $B_z$ and moved equatorward by approximately $8^\circ$ from $B_z = 5\gamma$ to $B_z = -5\gamma$. The diagram also illustrates that the width of the polar cusp region increases with increasing $B_z$ magnitude; the cusp is about $4^\circ$ wide in latitude during southward interplanetary magnetic field and $7^\circ$ wide during strong northward fields. This statistical study reveals the predictability of the latitudinal position of the polar cusp region under known interplanetary magnetic field condition. The above two pioneer works on the polar cusp variation set up the scenario for studying the effect of the interplanetary magnetic field to the polar cap regions.

The midday part of the auroral oval is located near the foot of the field lines threading the high altitude polar cusp (i.e., the cleft) near the magnetopause *(Heikkila and Winningham, 1971; Frank, 1971)*. The extent of the equatorward motion of the midday aurora can be used as a measure of the amount of the magnetic flux transferred from the dayside magnetosphere into the magnetotail by a southward directed interplanetary magnetic field. The polar orbiting USAF DMSP satellites have made routine observations of the global auroral distribution since 1973, and the dayside auroral oval over the southern polar region is recorded during the southern winter months *(Akasofu,*

*1976).* It was found that continuous discrete auroral arcs extending toward the noon sector from both morning and afternoon sectors of the auroral oval abruptly truncate in the midday sector. Thus, the instantaneous optical auroral oval does not appear to extend continuously across the dayside auroral oval *(Snyder and Akasofu, 1976; Cogger et al., 1977;* and *Dandekar and Pike, 1978).* Figure 3 illustrates an example of this gap along the midday auroral oval. The latitudinal position of the midday auroral oval can be inferred from the location of this midday auroral gap, even though the detailed relationship between the auroral gap and the polar cusp region is not yet clear. From more than one hundred orbits of dayside auroral observations, *Dandekar (1979)* found that the average position of the midday auroral gap is at 75.4° ± 1.7° corrected geomagnetic latitude, and that individual gap locations have a significant dependence on the magnitude of the north-south component of the interplanetary magnetic field, as demonstrated in Figure 4. The hourly average value of the interplanetary $B_z$ component observed 45 minutes before the auroral observation was used to correlate with the auroral gap latitude, and the least square linear fit for the $-B_z$ domain is represented by the line $\lambda = 76.1° + 0.59\ B_z$ with a correlation coefficient of only 0.59. A general trend of equatorial motion of the dayside auroral gap with southward interplanetary magnetic field is observed, but with substantial scatter of the individual shift of about 0.6° per each gamma of the southward interplanetary magnetic field obtained from the dayside auroral gap agrees with the OGO-4 cusp particle precipitation measurements. This large scattering is likely due to the effect of magnetospheric substorm activity, as well as the utilization of the hourly average of $B_z$ at 45 minutes before the dayside auroral observation.

## III. SUBSTORM EFFECTS ON THE POLAR CUSP LATITUDE

The equatorward shifts of the dayside auroral and cusp regions in association with magnetospheric substorms have been established by a number of statistical studies *(Feldstein, 1973; Chubb and Hicks, 1970; Burch, 1970; Hoffman, 1972; Winningham, 1972; McDiarmid et al., 1972; and others)*. Thus, it is important to separate the effects of the substorm activity from the effects of the interplanetary magnetic field on the latitudinal variations of the polar cusp and the auroral oval. *Yasuhara et al. (1973)* examined the position of the polar cusp using consecutive ISIS-1 satellite orbits and simultaneous interplanetary magnetic field and substorm activity as represented by AE index. They found that the polar cusp (i.e., the dayside auroral oval) shifts equatorward as the interplanetary $B_z$ component turns southward and the substorm activity increases, and shifts poleward as substorm activity subsides and $B_z$ returns northward. As illustrated in Figure 5, the shifts take place on a time scale less than the 1 to 2 hours of the satellite's orbital period.

A more conclusive study revealing separate controls of the polar cusp position by the interplanetary magnetic field and by the substorm was conducted by *Kamide et al. (1976)*. By reexamining the equatorial edge of the polar cusp observed by OGO-4, a latitudinal difference between the polar cusp location during the geomagnetically quiet periods and that during the magnetospheric substorm was found. In Figure 6, most of the crossings detected during substorms lie below those during quiet times, regardless of the magnitude of the interplanetary $B_z$ component. Therefore, the southward interplanetary magnetic field causes an equatorward movement of the polar cusp region, and the occurrence of magnetospheric substorms adds a noticeable further contribution to the equatorward shift. The substorm-caused equatorial motion of the polar cusp is consistent with the equatorward drift of the midday aurora during the expansive phase of substorms observed from the South Pole station *(Akasofu, 1972)*. It has generally been thought that the substorm is a manifestation of a suddenly-enhanced reconnection of magnetic flux in the magnetotail to convert open geomagnetic field lines into closed field lines returning to the dayside magnetosphere. Thus, during substorms the number of open geomagnetic field lines from the polar cap should be reduced and a poleward motion of the polar cusp (i.e., the dayside auroral oval) is expected.

It is important to point out that the observed equatorward displacement of the polar cusp and the midday aurora do not seem to agree with this popular concept of the magnetospheric substorm *(Akasofu, 1977)*.

## IV. MOTIONS OF THE POLAR CUSP

The changes of the cusp position can be determined statistically by one point measurements using the polar orbiting satellite observations, but the actual "motions", response time and velocity of the polar cusp require a continuous monitoring. The projection of the polar cusp upon the polar ionosphere can be easily monitored by suitably located all-sky cameras and ionosondes as the dayside auroral oval and the F layer irregularity zone, respectively *(Winningham et al., 1973; Pike, 1971, 1972)*. *Pike et al. (1974)* compared airborne observations of the equatorward boundary of the F layer irregularity zone and discrete auroras obtained by the AFGL flying ionospheric laboratory with the corresponding interplanetary magnetic field. It was found that midday auroras and the equatorward boundary of the F layer irregularity zone moved equatorward about 10-30 minutes after a southward turning of the interplanetary magnetic field and moved poleward about 15-50 minutes after a northward turning of the field. Figure 7 illustrates the events observed on December 21, 1968.

From the ground-based all-sky camera data at the South Pole Station (geomagnetic latitude of $-74^{\circ}$), which is under the midday part of the auroral oval near 16 UT each day, *Horwitz and Akasofu (1977)* reported that within 10-15 minutes after a sharp southward (or northward) change of the interplanetary magnetic field, the dayside auroral oval moves equatorward (or poleward) as shown in Figure 8. It is interesting to note that even the fine fluctuations of the interplanetary field are reflected by the motions of the discrete auroras. The motion of the midday auroral oval can be used to calculate the magnetospheric response to the $B_z$ variations by assuming an approximately exponential response which is represented by the equation

$$\lambda(t) = \lambda_f + (\lambda_i - \lambda_f)\, e^{-t/\tau}$$

where t is the time after the initial response of the aurora to the change in the interplanetary field, $\lambda(t)$ is the latitude of the aurora at time t, $\lambda_i$ and $\lambda_f$ are the initial and final latitudes of the aurora, and $\tau$ is the time constant for exponential response. The curve fitting procedure, as shown in Figure 9, indicates that the average exponential time constant is about 17 minutes.

On the other hand, the motion of the polar cusp region examined from the ground-based observations does not always show a simple polar cusp variation with a change of the interplanetary magnetic field. From a study of 5 days of ionogram data from two high latitude stations near or under the polar cusp, *Stiles et al. (1977)* found that the ionospheric manifestation of the cusp is very complex and dynamic. No clear relation between the position of the polar cusp and the direction of the interplanetary magnetic field was obtained in these 5 days of observations. Events both agreeing with and contrary to the earlier conclusions were detected.

## V. EFFECTS OF NIGHTSIDE AURORAL OVAL

The observation of an equatorward shift of the dayside polar cusp position does not conclusively indicate a larger polar cap (i.e., more open geomagnetic field lines), unless the latitude of the nightside auroral oval also moved simultaneously equatorward. A time delay of ~ 50 minutes between the southward turning of the interplanetary magnetic field and the onset of substorms was reported *(Arnoldy, 1971; Foster et al., 1971)*. Examining all-sky camera data from nine different stations collected during and after IGY, *Vorobjev et al. (1976)* found that there was a pronounced equatorward motion of the entire auroral oval, usually at about 50 minutes before the expansive phase of the auroral substorm. Thus, the observed equatorward shift of the auroral oval, before the substorm activity, is suggested in association with the onset of the southward interplanetary magnetic field. Figure 10 illustrates that the equatorward shift of the evening auroral oval is related to the change of the interplanetary field direction and the onset of the auroral motion coincides with the sudden decrease of the $B_z$ component.

The auroral oval motion near the midnight sector was revealed by a statistical study of the equatorial boundary of the auroral electron precipitation ($E_e$ > 100 eV) detected by ISIS-1 and 2 satellites *(Kamide and Winningham, 1977)*. The equatorial boundary of the nightside diffuse auroral precipitation during periods of the southward interplanetary field was observed at lower latitudes than during the northward interplanetary field. Table 1 lists the results on the rate of equatorward motion as a function of $B_z$ magnitude for each hour interval of the local time sectors from 20 LT to 04 LT. In general, the auroral oval moves about 0.6° for each gamma of $B_z$ variation similar to the latitudinal motion of the dayside polar cusp *(Burch, 1973)*. From these observations, we are certain that the entire auroral oval responds simultaneously and also coherently with the change of the interplanetary magnetic field direction.

**TABLE 1**

**Statistical Variations of the Nightside Auroral Electron (> 100 eV) Precipitation Boundary With the Interplanetary Bz Component (Kamide and Winningham, 1977)**

| MLT Interval | $\alpha$ | $\Lambda_o$ (degree) | Correlation Coefficient |
|---|---|---|---|
| 20 - 21 | 0.48 | 65.8 | 0.68 |
| 21 - 22 | 0.50 | 65.7 | 0.61 |
| 22 - 23 | 0.49 | 65.4 | 0.71 |
| 23 - 24 | 0.46 | 64.5 | 0.51 |
| 00 - 01 | 0.74 | 63.4 | 0.56 |
| 01 - 02 | 0.76 | 64.1 | 0.53 |
| 02 - 03 | 0.63 | 63.3 | 0.42 |
| 03 - 04 | 1.38 | 64.6 | 0.67 |
| Average | 0.60 | 64.5 | 0.55 |

$$\Lambda^{\circ} (B_z) = \Lambda_o + \alpha B_z$$

where $B_z$ is in unit of gamma

## VI. DMSP AURORAL OVAL OBSERVATIONS

The problem of one-point determination of the oval location has been resolved to a significant extent by using the auroral imagery technique onboard the polar orbiting satellites *(Anger et al., 1973; Pike and Whalen, 1974)*. These instruments provide images of the entire or part of the global auroral display over the dark polar region once each orbit (of ~ 100 minutes or longer) *(Akasofu, 1974; 1976)*. This simultaneous observation of the auroral oval gives a more definitive "measure" of the polar cap size. Methods of using global auroral displays to examine the variations of the polar cap in association with the interplanetary field are discussed here. A straightforward way is to identify the equatorial edge of the auroral oval at a specific local time interval and then correlate its latitude with the corresponding interplanetary field condition. *Lui (private communication)* used 31 ISIS-2 auroral images to locate the positions of the boundary of diffuse aurora at the 21 MLT sector and established the relation $\Lambda(B_z) = 65.6^\circ + 0.55\ B_z$ which is very similar to that determined from particle measurements shown in Table 1 *(Kamide and Winningham, 1977)*.

Another method is to determine the size of the polar cap from the global auroral picture. Figure 11 is an example of the quiet auroras observed over the northern polar region by a dawn-dusk DMSP satellite. The ground projection of this auroral display is shown on the bottom panel giving a perspective display which enables us to determine the size of the polar cap. In order to use them efficiently, we have to define some quantitative representations of the global auroral distribution. *Holzworth and Meng (1975)* described a curve fitting procedure for a mathematical representation of the auroral oval. They fitted a seven parameter Fourier Series to the DMSP auroral pictures and introduced two quantitative parameters to indicate the dynamics of the auroral oval, namely the radius of an off-set (from the geomagnetic pole) circle indicating the size of the auroral oval and the "center" of this circle indicating the location of the auroral oval. Fitting this curve to more than 50 DMSP auroral images of bright extended quiet auroras, *Meng et al. (1977)* showed that the quiet global discrete auroral distributions indeed have the shape of an off-centered circle in corrected geomagnetic latitude and local time coordinates, instead of the expected oval shape. Figure 12 is an example of the circle fitting of several data points scaled along the quiet auroral arc in Figure 11. The offset circle

has its center position at 6.06° co-latitude along the 2318 MLT meridian and a radius of 14.56° co-latitude. It can be seen that the observed extended auroral arc is represented very well by this offset circle. The average deviation of 0.22° between the scaled auroral locations and the fitted values is smaller than the errors of scaling and coordinate transformation. Thus, the radius and the center location of a fitted circle can be used quantitatively to represent variations of the global auroral configuration.

Using observations during quiet auroral displays, *Holzworth and Meng (1975)* found a linear relation between the radius of the auroral circle (i.e., the size of the polar cap) and the hourly averaged magnitude of the interplanetary $B_z$ component (Figure 13). The size of the auroral circle (or oval) increases approximately 0.9 degrees of co-latitude for every 1.0 gamma decrease in $B_z$ with a rather small scattering. However, a much larger scatter occurred when data from a broader range of auroral activities were included (Figure 14). This preliminary result showed that the radius of the auroral circle varying with values of $B_z$ by

$$R = 20.5^\circ - 1.25\ B_z$$

where R is in units of degrees of co-latitude and $B_z$ is in gammas.

## VII. EFFECTS OF THE $B_x$, $B_y$ COMPONENTS

The importance of the $B_z$ component in the energy transfer process from the interplanetary space into the magnetosphere was emphasized in the simplified 2-dimensional field line reconnection model proposed by *Dungey (1961)*. However, the presence of the $B_x$ and $B_y$ components of the interplanetary magnetic field has been generally ignored in the earlier studies until the recent theoretical considerations of the three dimensional reconnection *(Cowley, 1973; Stern, 1973; Gonzalez and Mozer, 1974;* and *Mozer et al., 1974)*. Figure 15 illustrates the qualitative interaction of the geomagnetic field with an assumed purely dusk to dawn uniform interplanetary magnetic field *(Cowley, 1973)*. The diagram represents the field configuration in the dusk-dawn meridian plane viewed from the sun, the neutral points located in the morning side of the northern hemisphere and in the evening side of southern hemisphere, respectively. The orientation of the reconnection line which traces out the location of the field line merging coincides with the intersection between the magnetopause and the ecliptic plane when the interplanetary field is purely southward. However, the reconnection line no longer has this simple geometry in the presence of the $B_y$ component. Its orientation is highly dependent on the $B_y$ direction of the imposed interplanetary field. Figure 16 illustrates two orientations of the reconnection line (LL') viewed from the sun to the magnetosphere in a pure dawn to dusk ($B_y > 0$) and pure dusk to dawn ($B_y < 0$) interplanetary magnetic field *(Mozer et al., 1974)*. The reconnection with the $B_y$ component of the interplanetary magnetic field causes a displacement of the entire polar cap toward dawn (or dusk) in the northern hemisphere and toward dusk (or dawn) in the southern hemisphere when $B_y > 0$ (or $B_y < 0$) as discussed by *Stern (1973), Gonzalez and Mozer (1974),* and *Mozer et al. (1974)*. Figure 17 shows the distribution of the electric field equipotentials (solid lines) and the northern polar cap boundary (dashed circle) based on an open magnetospheric model calculated by *Stern (1973)*. Diagram (a) corresponds to a condition of the pure dawn to dusk interplanetary field ($B_y > 0$), (b) $B_y > 0$ as well as $B_x < 0$ condition, (c) $B_y > 0$, $B_x < 0$ and $B_z < 0$ condition, and (d) $B_y > 0$, $B_x < 0$ and $B_z > 0$ condition. The effects of the different interplanetary magnetic field orientations on the northern polar cap are clearly shown. A positive interplanetary $B_y$ field caused a dawnward shift of the entire polar cap, the positive $B_z$ produced a small polar cap and a negative $B_x$ moves the northern polar cap tailward. *Gonzalez and Mozer (1974)* also concluded that the northern (southern) polar cap should shift tailward (sunward) when $B_x$ is negative, whereas for $B_x > 0$ the opposite should occur.

Displacements of the polar cap can be determined from the center location of the auroral circle fitted to the DMSP auroral pictures. A preliminary examination of the many auroral pictures revealed indications of the shift of the entire polar cap under different interplanetary $B_x$ and $B_y$ directions. Figure 18 shows the center locations of the auroral displays observed over both northern and southern polar regions with the corresponding hourly interplanetary field $B_y$ is negative and dawnward when $B_y > 0$. This trend is in agreement with the theoretical considerations of *Stern (1973)* and *Gonzalez and Mozer (1974)*. Over the southern polar cap, there is no clear trend between these two parameters. Figure 19 illustrates the relation between the centers of the auroral displays and the values of the interplanetary $B_x$ component. In the northern polar region, the polar cap moved tailward when $B_x$ was positive and sunward for negative $B_x$. In the southern polar cap a tailward shift was also detected when $B_x$ was negative. The trends of the polar cap displacements with $B_x$ component of the interplanetary fields are exactly opposite to the directions expected from the theoretical models.

## VIII. SUMMARY

Based on various types of satellite, ground-based and airborne observations, there is no doubt that the configuration of the polar cap is sensitive to the orientation of the interplanetary magnetic field. Its north-south component controls the size of the polar cap, and its $B_x$ and $B_y$ components affect the orientation (i.e., location of the center of the fitted circles) of the polar cap. Table 2 summarizes the variation of the polar cap size with the north-south component of the interplanetary field. The rate of the oval size varies from about 0.5 degrees to more than 1 degree per one gamma of $B_z$ change. This difference among observations may be attributed to the utilization of different definitions in averaging the interplanetary magnetic field. For example, *Burch (1973)* averaged $B_z$ data over a time interval of 45 minutes prior to the observation of the polar cusp crossing; whereas *Holzworth and Meng (1975)* as well as the Figure 14 in this article used the hourly averaged values given by the National Space Science Data Center's Interplanetary Magnetic Field Data Book at the time of the DMSP auroral oval observation. Refined studies are certainly needed for obtaining a more consistent and precise rate of change. The motions of polar cap expansion and contraction as well as the response time of the magnetosphere to the southward and northward turnings of the interplanetary magnetic field were examined. In general, the motion of the auroral oval starts about 10 to 30 minutes after the turning of the interplanetary magnetic field, and a speed of the motion of $\sim 0.1^\circ$ in latitude per minute is obtained. These quantitative parameters are essential in any detailed modelling of interaction and energy transfer processes between the solar wind and the magnetosphere. More systematic and detailed observations of these quantitative parameters are needed in the future.

The responses of the magnetosphere to the $B_x$ and $B_y$ components of the interplanetary field have been sparsely studied. Most of the earlier studies of the $B_y$ component effect were concerned with the polar cap electric field distribution instead of the polar cap configuration. The DMSP auroral pictures reveal that the location of the entire auroral oval (i.e., the polar cap) changes with the interplanetary magnetic field. Table 3 summarizes the orientations of the oval shift compared with the expected changes from theoretical considerations. Over the northern polar region, the auroral oval

moved toward the dawn side (duskside) when the interplanetary magnetic field had a positive (negative) $B_y$ component. These motions of the polar cap are in agreement with the model calculations *(Stern, 1973; Gonzalez and Mozer, 1974)*. Over the southern polar region, the direction of the oval motion was not conclusive from this set of DMSP data.

The effect of the interplanetary field $B_x$ component was also examined. Over the northern hemisphere, the polar cap moves sunward when the interplanetary field is pointing away from the Sun ($B_x < 0$) and tailward for a positive $B_x$ direction. The observations over the southern polar cap shows a tailward shift while $B_x$ is negative. These variations of the polar cap orientation (i.e., the location) with the interplanetary field $B_x$ component do not agree with directions expected in model calculations of *Stern (1973)* and *Gonzalez and Mozer (1974)*. Since the $B_x$ variation discussed here is only a preliminary result and also the first such observation, it is not clear yet whether the three dimensional interaction models referenced above should be modified. From this review, it is rather clear that in order to understand the three dimensional interaction between the solar wind and the magnetosphere, especially the energy transfer process, further studies of the quantitative relation of the polar region responses to the variations of the interplanetary magnetic field are needed. The effect of the interplanetary $B_x$ and $B_y$ components to the magnetosphere requires special attention.

## TABLE 2

## OVAL SIZE AND IMF $B_z$ MAGNITUDE

| | Observation | Rate | $B_z$ Range | Local Time Sector |
|---|---|---|---|---|
| Burch (1973) | Poleward Edge | ~ 0.8/γ | $-B_z$ | Dayside Cusp |
| | Equatorward Edge | ~ 0.5/γ | | |
| Dandekar (1979) | | ~ 0.6/γ | $-B_z$ | Dayside Oval Gap |
| Kamide and Winningham (1977 | Equatorial Edge | ~ 0.5/γ | All $B_z$ | Nightside Auroral Oval |
| Holzworth and Meng (1975) Also Figure 14 | Auroral Circle Radius | ~ 1/γ | All $B_z$ | Mostly Nightside Discrete Oval |

## OVAL EXPANSION SPEED AND RESPONSE TIMES

| | | |
|---|---|---|
| Burch (1972) | < 45 minutes, ~ 0.1° /min. | OGO-4 Particle Observation |
| Pike et al., (1974) | ~ 10 - 30 Minutes | Ionospheric and Auroral Observations |
| Vorobjev et al., (1976) | ~ 10 - 20 Minutes | All-Sky Camera Data |
| Horwitz and Akasofu (1977) | Exponential time constant ~ 15 - 20 minutes. | All-Sky Camera Data |

## TABLE 3

## OVAL ORIENTATION SHIFT WITH IMF $B_y$, $B_x$

| IMF | Observation | Observed Shift | Modelling* |
|---|---|---|---|
| $B_y < 0$ | Northern Cap | Duskward | Duskward |
| | Southern Cap | (?) | Dawnward |
| $B_y > 0$ | Northern Cap | Dawnward | Dawnward |
| | Southern Cap | (?) | Duskward |
| $B_x < 0$ | Northern Cap | Sunward | Tailward |
| | Southern Cap | Tailward | Sunward |
| $B_x > 0$ | Northern Cap | Tailward | Sunward |
| | Southern Cap | (?) | Tailward |

*Stern (1973); Gonzalez and Mozer (1974)

REFERENCES


Akasofu, S. I.,: 1972, *J. Geophys. Res., 77,* 2303

Akosofu, S. I.,: 1974, *Space Sci. Rev., 16,* 617

Akasofu, S. I.,: 1976, *Space Sci. Rev., 19,* 169

Akasofu, S. I.,: 1977, *Physics of Magnetospheric Substorms, D. Reidel Pub. Co., Dordrecht, Holland*

Anger, C. D., Fancott, T., McNally, J. and Kerr, M. S.,: 1973, *Appl. Optics., 12,* 1753

Arnoldy, R. L.,: 1971, *J. Geophys. Res., 76,* 5189

Burch, J. L.,: 1970, *In the Polar Ionosphere and Magnetospheric Processes, Edited by G. Skovli, Gordon and Breach, New York*

Burch, J. L.,: 1972, *J. Geophys. Res., 77,* 6696

Burch J. L.,: 1973, *Radio Sci., 8,* 955

Burch, J. L.,: 1974, *Rev. of Geophys. and Space Physics., 12,* 363

Chubb, T. A. and Hicks, G. T., 1970: *J. Geophys. Res., 75,* 1290

Cogger, L. L., Murphree, J. S., Ismail, S. and Anger, C. D.,: 1977, *Geophys. Res. Lett., 4,* 413

Cowley, S. W. H.,: 1973, *Radio Sci., 8,* 903

Dandekar, B. S.,: 1979, *Private Communication*

Dandekar, B. S., and Pike, C. P.,: 1978, *J. Geophys. Res., 83,* 4227

Dungey, J. W.,: 1961, *Phys. Rev. Lett., 6,* 47.

Feldstein, Y. I.,: 1973, *J. Geophys. Res., 78,* 1210

Foster, J. C., Fairfield, D. H., Ogilive, K. W., and Rosenberg, T. L.,: 1971, *J. Geophys. Res., 76,* 6971

Frank, L. A.,: 1971, *J. Geophys. Res., 76,* 5202

Gonzalez, W. D., and Mozer, F. S.,: 1974, *J. Geophys. Res., 79,* 56

Heikkila, W. J., and Winningham, J. D.,: 1971, *J. Geophys. Res., 76,* 883

Hoffman, R. A.,: 1972, *in K. Folkstad (ed.) Magnetosphere - Ionosphere Interactions, Universites Forlaget, Oslo, Norway,* 117

Holzworth, R. H., and Meng, C. I.,: 1975, *J. Geophys. Res. Lett., 2,* 377

Horwitz, J. L., and Akasofu, S. I.,: 1977, *J. Geophys. Res., 82,* 2723

Kamide, Y., Burch, J. L., Winningham, J. D., and Akasofu, S.-I.,: 1976, *J. Geophys. Res., 81,* 698

Kamide, Y. and Winningham, J.D., 1977, J. Geophys. Res., 82, 5573.

McDiarmid, I. G., Burrows, J. R., and Wilson, M. D.,: 1972: *J. Geophys. Res., 77,* 1103

Meng, C.-I., Holzworth, R. H., and Akasofu, S. I.,: 1977, *J. Geophys. Res., 82,* 164

Mozer, R. S., Gonzalez, W. D., Bogott, R., Kelley, M. C., and Schulta, S.,: 1974, *J. Geophys. Res., 79,* 56

Pike, C. P.,: 1971, *J. Geophys. Res., 76,* 7745

Pike, C. P.,: 1972, *J. Geophys. Res., 77,* 6911

Pike, C. P., and Whalen, J. A.,: 1974, *J. Geophys. Res., 79,* 985

Pike, C. P., Meng, C.-I., Akasofu, S.-I., and Whalen, J. A.,: 1974, *J. Geophys. Res., 79,* 5129

Russell, C. T.,: 1979, *Space Sci. Rev., this issue*

Russell, C. T., Chappel, C. R., Montgomery, M. D., Neugebauer, M., and Scarf, F. L.,: 1971, *J. Geophys. Res., 76,* 6743

Snyder, A. L., and Akasofu, S.-I.,: 1976, *J. Geophys. Res., 81,* 1799

Stiles, G. S., Hones, E. W. Jr., Winningham, J. D., Lepping, R. P., and Delana, B. S.,: 1977, *J. Geophys. Res., 82,* 67

Stern, D. P.,: 1973, *J. Geophys. Res., 78,* 7292

Vorobjev, V. G., Starkov, G. V., and Feldstein, Y. I.,: 1976, *Planet Space Sci., 24,* 955

Winningham, J. D.,: 1972, *in "Earth's Magnetospheric Processes", B. M. McCormac (ed.), 68, D. Reidel Publ. Co., Dordrecht - Holland*

Winningham, J. D., Akasofu, S.-I., Yasuhara, F., and Heikkila, W. J.,: 1973, *J. Geophys. Res., 78,* 6579

Yasuhara, F., Akasofu, S.-I., Winningham, J. D., and Heikkila, W. J.,: 1973, *J. Geophys. Res., 78,* 7286

FIGURE CAPTIONS

FIGURE 1 The latudinal location of polar cusp as a function of the time span following sharp onsets of southward interplanetary magnetic field. $\Delta\Lambda$ is the difference between the latitude of the observed lower boundary of polar cusp and the expected boundary. The average southward component of the interplanetary magnetic field between the onset of southward field and the observation is given for each point, together with the ratio of southward flux eroded into the tail to the flux brought to the front of the magnetosphere (Burch, J. L.,: 1972, *J. Geophys. Res.*, *77*, 6696).

FIGURE 2 Locations of the poleward (circles) and equatorward (dots) boundaries of dayside cusp electron precipitation for 45 minute $B_z$ averages. (Burch, J. L.,: 1973, *Radio Sci.*, *8*, 956).

FIGURE 3 DMSP auroral picture (in negative) of the dayside (bottom) and midnight auroral display. Note the discontinuity of the auroral oval (gap) between 09 MLT and 12 MLT near the noon meridian. (Courtesy of B. S. Dandekar).

FIGURE 4 The dependence of the corrected geomagnetic latitude of the center of the midday auroral gap (or of the ray structure) with the interplanetary $B_z$ component. The least equare straight line was fitted to data for negative values of IMF $B_z$. The $B_z$ are hourly values at about 45 minutes before the auroral observation. (Courtesy of B. S. Dandekar).

FIGURE 5 Example of polar cusp motion observed by ISIS-2 satellite. Both poleward and equatorward boundaries of the cusp are shown. Note the latitudinal variations of the cusp between successive orbits. (Yasuhara, F., Akasofu, S.-I., Winningham, J. D., and Heikkila, W. J.,: 1973, *J. Geophys. Res.*, *78*, 7286).

FIGURE 6 Location of the equatorward boundary of polar cusp electron precipitation. The data are divided into quiet periods and substorm times depending on the magnetic condition of the time when the cusp was observed. Note the clear separation between

quiet and substorm subgroups. (Kamide, Y., Burch, J. L., Winningham, J. D., and Akasofu, S.-I.,: 1976, *J. Geophys. Res.*, *81*, 698).

FIGURE 7 Interplanetary magnetic field north-south direction and the latitude of the equatorward boundary of the dayside F layer irregularity zone (FLIZ). Note the poleward motion of FLIZ near 03 UT and the equatorward motion near 0830 UT, in association with northward and southward turnings of the IMF, respectively. (Pike, C. P., Meng, C.-I., Akasofu, S.-I., and Whalen, J. A.,: 1974, *J. Geophys. Res.*, *79*, 5129).

FIGURE 8 Location of the dayside aurora observed at the south pole station together with the IMF $B_z$ component and AE index. Note the close relation between latitudinal variations of the dayside aurora and the variations of the $B_z$ component. (Horwitz, J. L., and Akasofu, S. -I.,: 1977, *J. Geophys. Res.*, *82*, 2723).

FIGURE 9 Exponential curve fitting of $\lambda(\tau)$ (see text) to the observed motions of the equatorward auroral boundary. The exponential response time constant $\tau$ is about 14 to 21 minutes. (Horwitz, J. L., and Akasofu, S.-I.,: 1977, *J. Geophys. Res.*, *82*, 2723).

FIGURE 10 Auroral oval dynamics and the IMF $B_z$ variations. The auroral dynamics were obtained from the ground-based all-sky camera data from Cape Cheluskin. Note the equatorward motion of the oval between 19 and 20 LT with association with a sharp southward turning of IMF near 19 LT. (Vorobjev, V. G., Starkov, G. V., and Feldstein, Y. I.,: 1976, *Planet Space Sci.*, *24*, 955).

FIGURE 11 An example of the quiet global auroral distribution from DMSP observations. The lower panel illustrates its ground projection showing the extent of the auroral display.

FIGURE 12 Auroral-circle fitting of the example shown in Figure 11 (see text). (Meng, C.-I., Holzworth, R. H., and Akasofu, S.-I.,: 1977, *J. Geophys. Res.*, *82*, 164).

FIGURE 13 Variation of the quiet auroral circle size and the simultaneous hourly IMF $B_z$ values. A linear relation between the size of the auroral circle and the north-south IMF component is clearly illustrated. (Holzworth, R. H., and Meng, C.-I.,: 1975, *J. Geophys. Res. Lett.*, *2*, 377).

FIGURE 14 Preliminary result of the auroral oval size and the hourly IMF $B_z$ component.

FIGURE 15 Magnetic field line configuration in the Y-Z plane under a uniform dusk to dawn interplanetary magnetic field. Note the locations of the neutral "points". (Cowley, S. W. H.,: 1973, *Radio Sci.*, *8*, 903).

FIGURE 16 Configuration of the reconnection line under two assumed uniform interplanetary magnetic fields, as viewed from the sun to the magnetosphere. The solid lines are interplanetary magnetic field lines, the dashed lines are terrestrial magnetic field lines on the magnetopause, line LL' is the reconnection line, and the white arrows indicate the direction of the post reconnection flows. (Mozer, F. S., Gonzalez, W. D., Bogott, R., Kelley, M. C., and Schultz, S.,: 1974, *J. Geophys. Res.*, *79*, 56).

FIGURE 17 Calculated equipotentials for an open magnetospheric model. The polar cap boundary is marked by dashed lines. (a) Corresponds to a uniform dawn to dusk IMF; (b) for $B_y > 0$ and $B_x < 0$; (c) $B_y > 0$, $B_x < 0$, $B_z < 0$ and (d) for $B_y > 0$, $B_x < 0$, $B_z > 0$. Note the displacement of the dashed circle from the origin for B, $B \pm 0$ conditions and changes of circle size due to $B_z$ variations (see text). (Stern, D. P.,: 1973, *J. Geophys. Res.*, *78*, 7292).

FIGURE 18 Dawn-dusk displacement of the auroral oval in association with the IMF $B_y$ component. Only the y coordinates of the center of auroral circles fitted to some DMSP auroral pictures are shown. A trend of dusk shift of auroral oval with $B_y < 0$, and dawn shift with $B_y > 0$ is observed over the northern polar region. A detailed analysis is in progress.

FIGURE 19 Sunward-tailward displacement of the auroral oval with variations of the IMF $B_x$ component. Tailward shift of the northern oval with $B_x > 0$ and sunward shift of the northern oval with $B_x < 0$ are observed. Over the southern polar region, a tailward shift of auroral oval with $B_x < 0$ may also exist. These are the preliminary results from a limited data set. The analysis is still in progress.

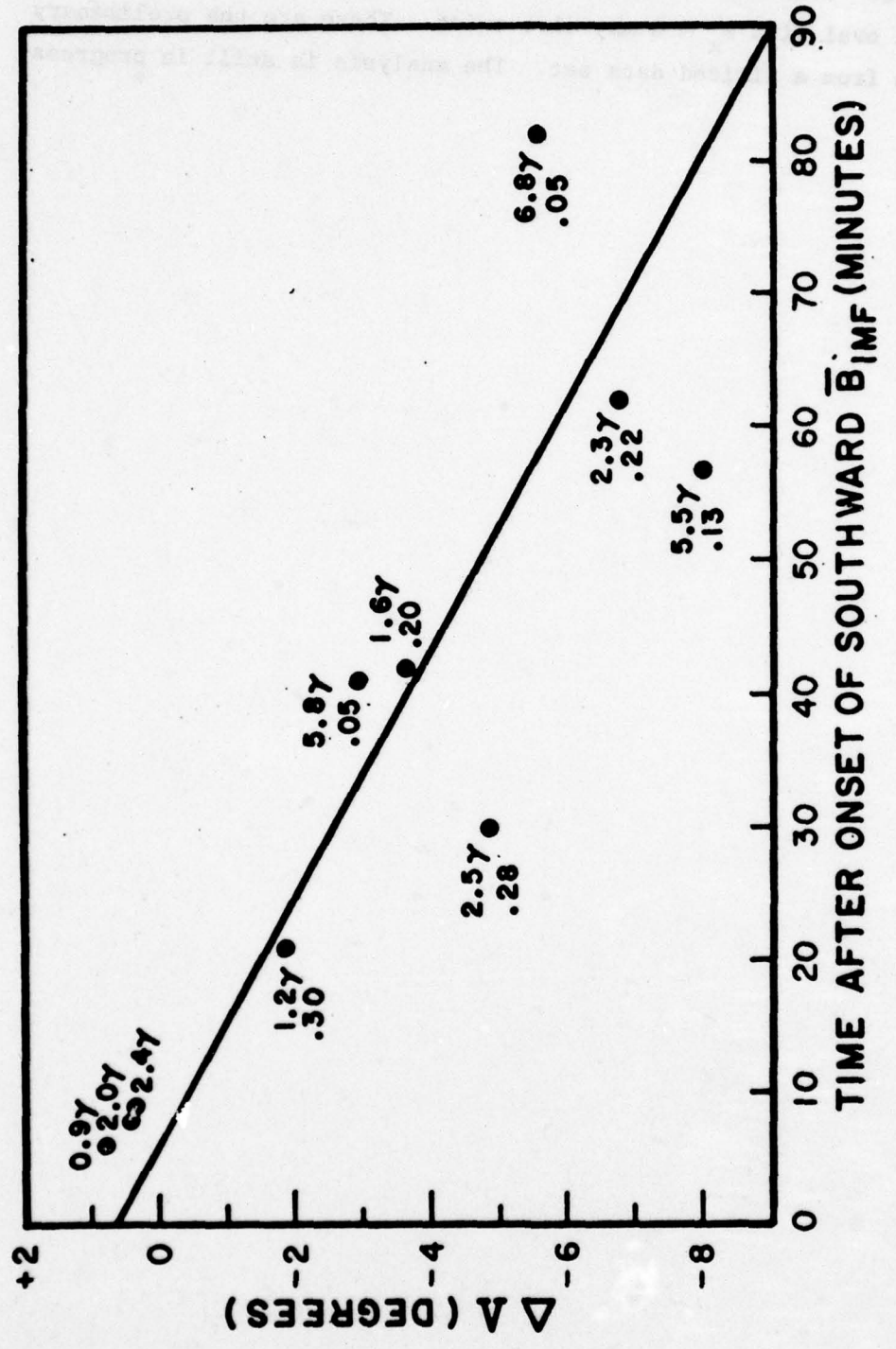
+2
0
-2
-4
-6
-8
Δ λ (DEGREES)
0
10
20
30
40
50
60
70
80
90
TIME AFTER ONSET OF SOUTHWARD $\bar{B}_{IMF}$ (MINUTES)
0.9γ
2.0γ
2.4γ
1.2γ
.30
2.5γ
.28
5.8γ
.05
1.6γ
.20
5.5γ
.13
2.3γ
.22
6.8γ
.05

FIGURE 1

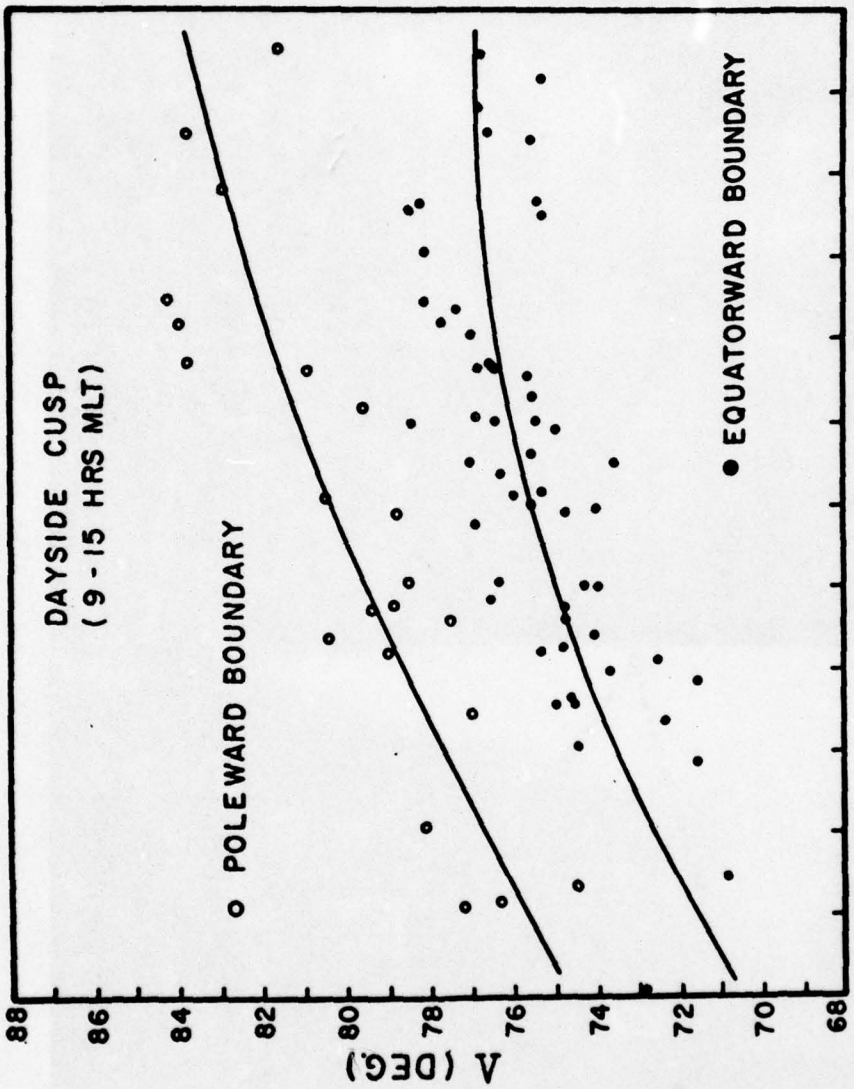
DAYSIDE CUSP
( 9 - 15 HRS MLT)
o POLEWARD BOUNDARY
• EQUATORWARD BOUNDARY
Λ (DEG)
88
86
84
82
80
78
76
74
72
70
68
-5 -4 -3 -2 -1 0 1 2 3 4 5
45 min. AVG $B_z$ (γ)

FIGURE 2

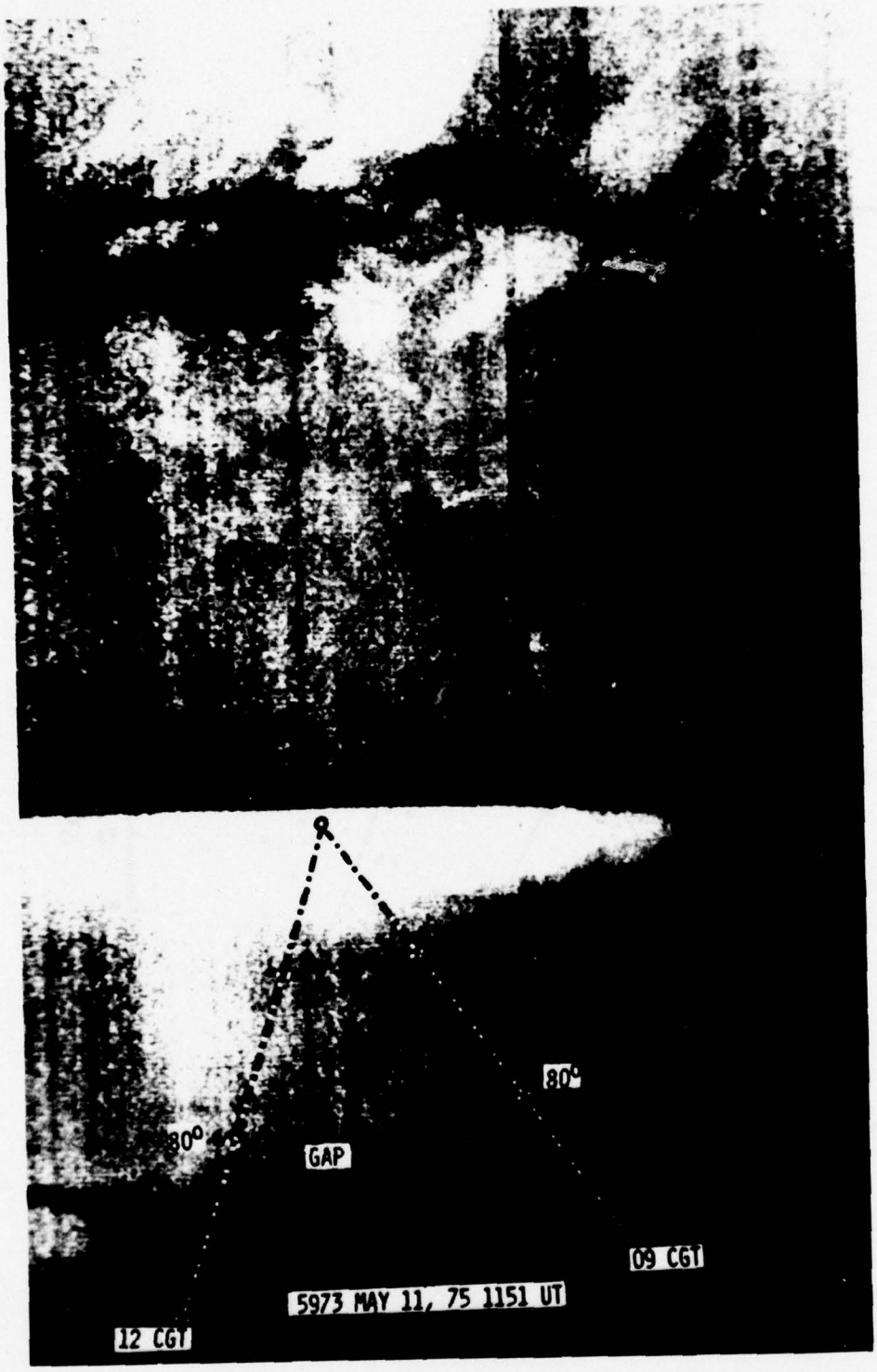


FIGURE 3

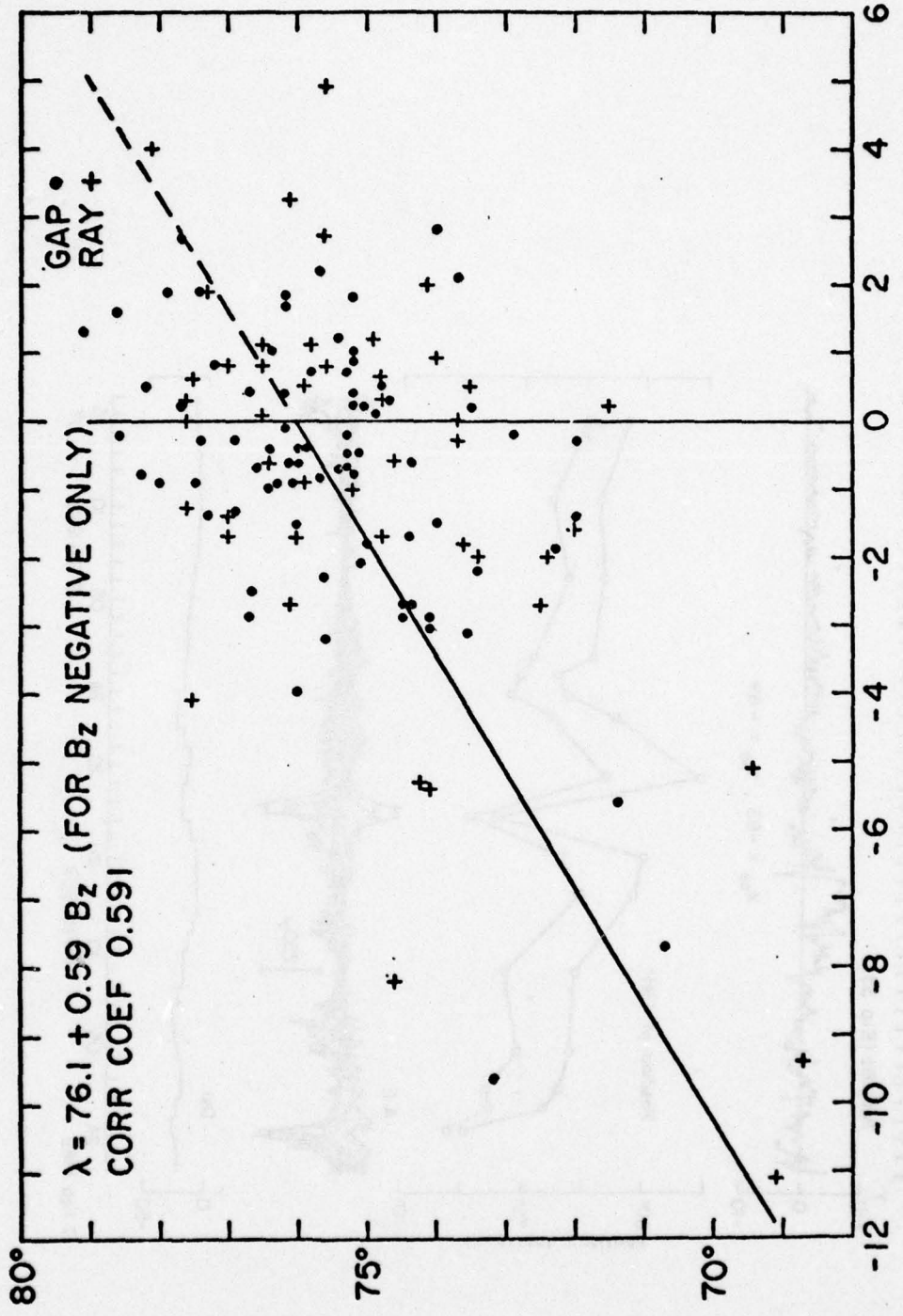
GAP •
RAY +
λ = 76.1 + 0.59 Bz (FOR Bz NEGATIVE ONLY)
CORR COEF 0.591
80°
75°
70°
CGL OF THE CENTER OF THE GAP/RAY
6
4
2
0
-2
-4
-6
-8
-10
-12
Bz (γ)

FIGURE 4

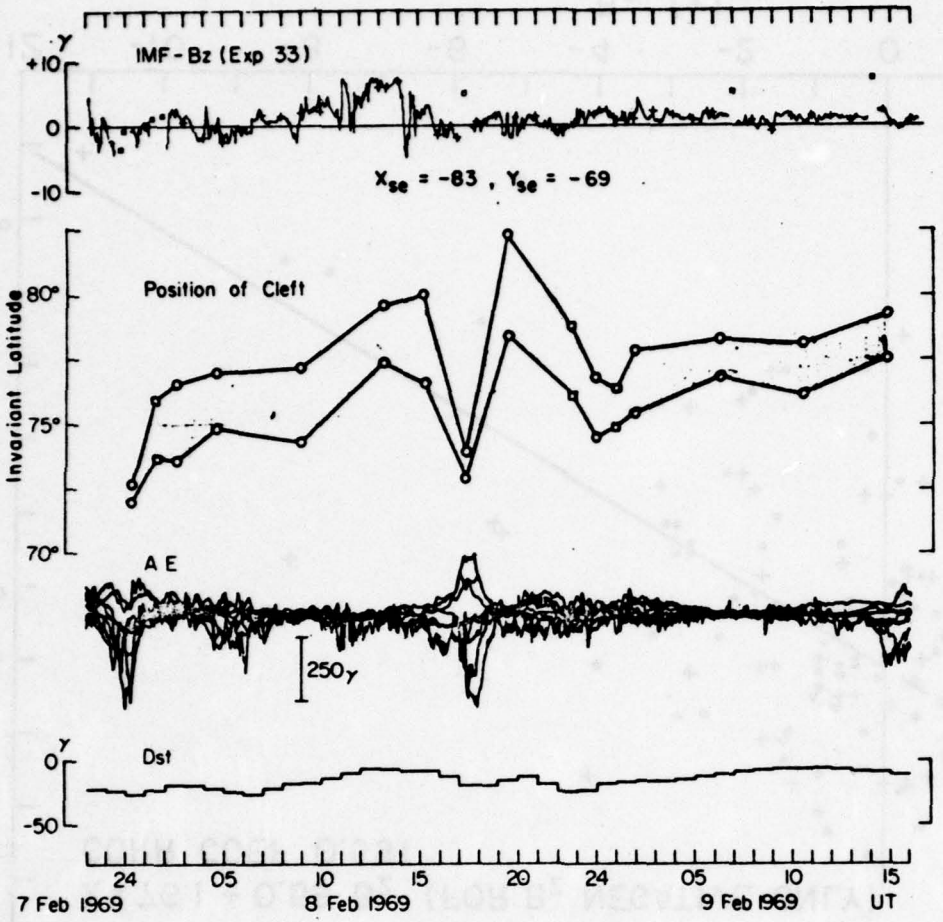
γ
+10
0
-10
IMF - Bz (Exp 33)
$X_{se}$ = -83 , $Y_{se}$ = -69
Invariant Latitude
80°
75°
70°
Position of Cleft
A E
250γ
γ
0
-50
Dst
24
05
10
15
20
24
05
10
15
7 Feb 1969
8 Feb 1969
9 Feb 1969
UT

FIGURE 5

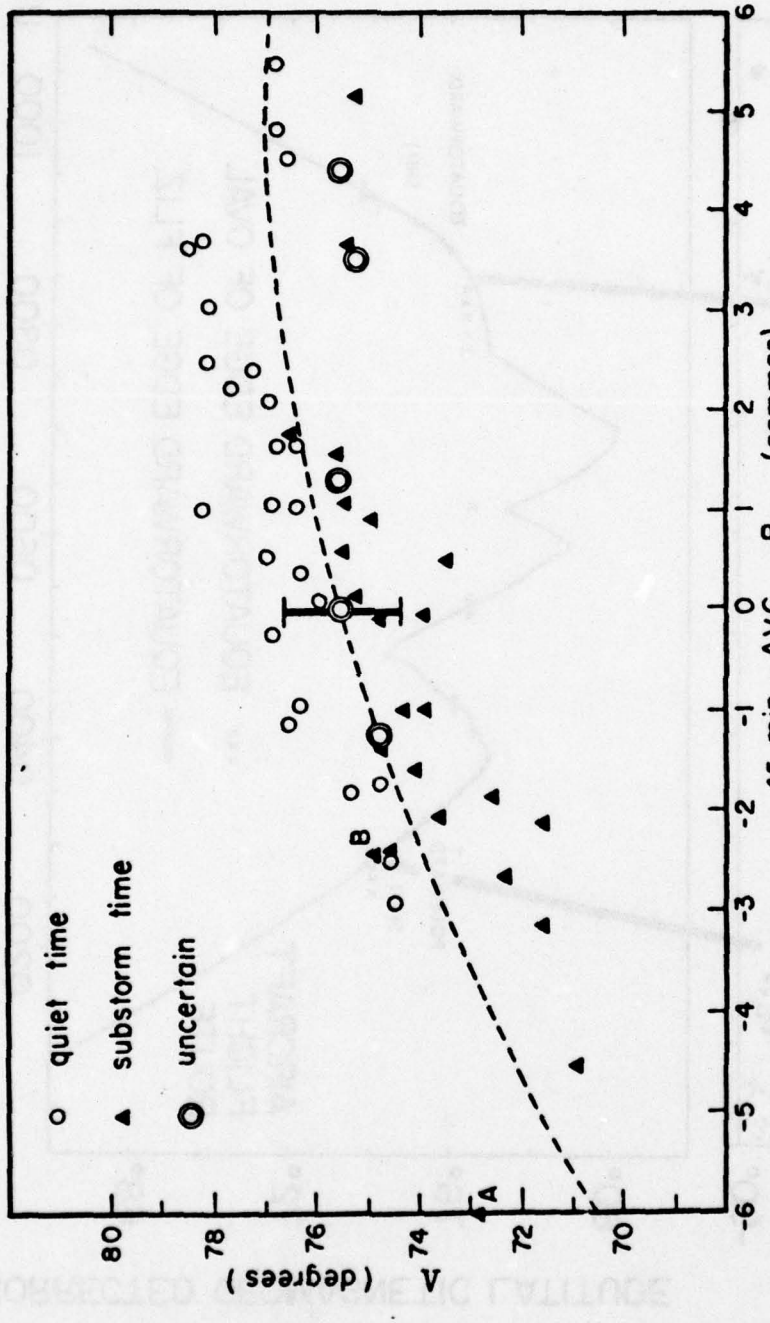
LOWER BOUNDARY OF CLEFT
quiet time
substorm time
uncertain
Λ (degrees)
80
78
76
74
72
70
A
B
-6
-5
-4
-3
-2
-1
0
1
2
3
4
5
6
45 min - AVG $B_z$ (gammas)

FIGURE 6

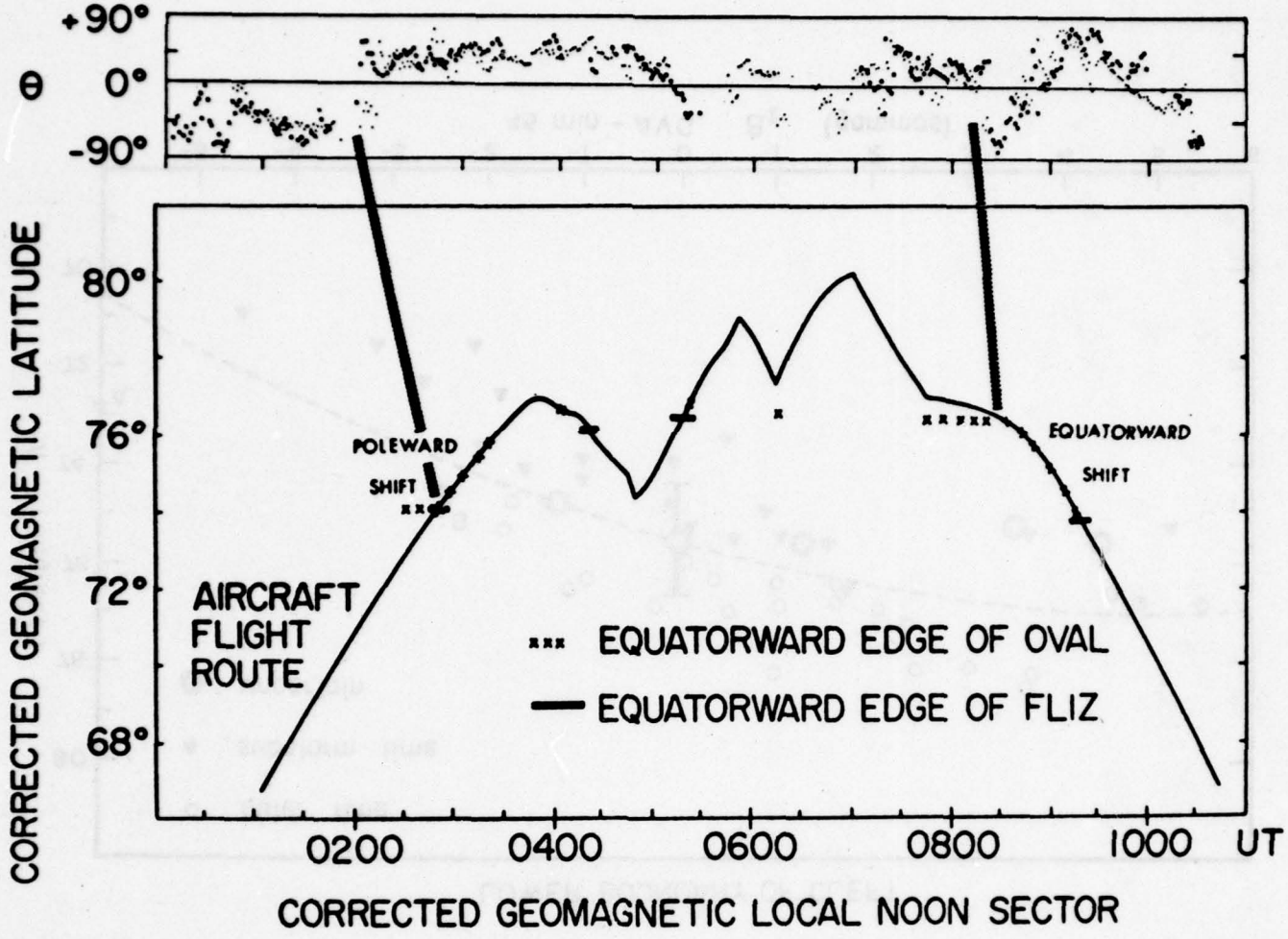
+90°
θ
0°
-90°
80°
76°
72°
68°
CORRECTED GEOMAGNETIC LATITUDE
POLEWARD
SHIFT
EQUATORWARD
SHIFT
AIRCRAFT
FLIGHT
ROUTE
EQUATORWARD EDGE OF OVAL
EQUATORWARD EDGE OF FLIZ
0200
0400
0600
0800
1000
UT
CORRECTED GEOMAGNETIC LOCAL NOON SECTOR

FIGURE 7

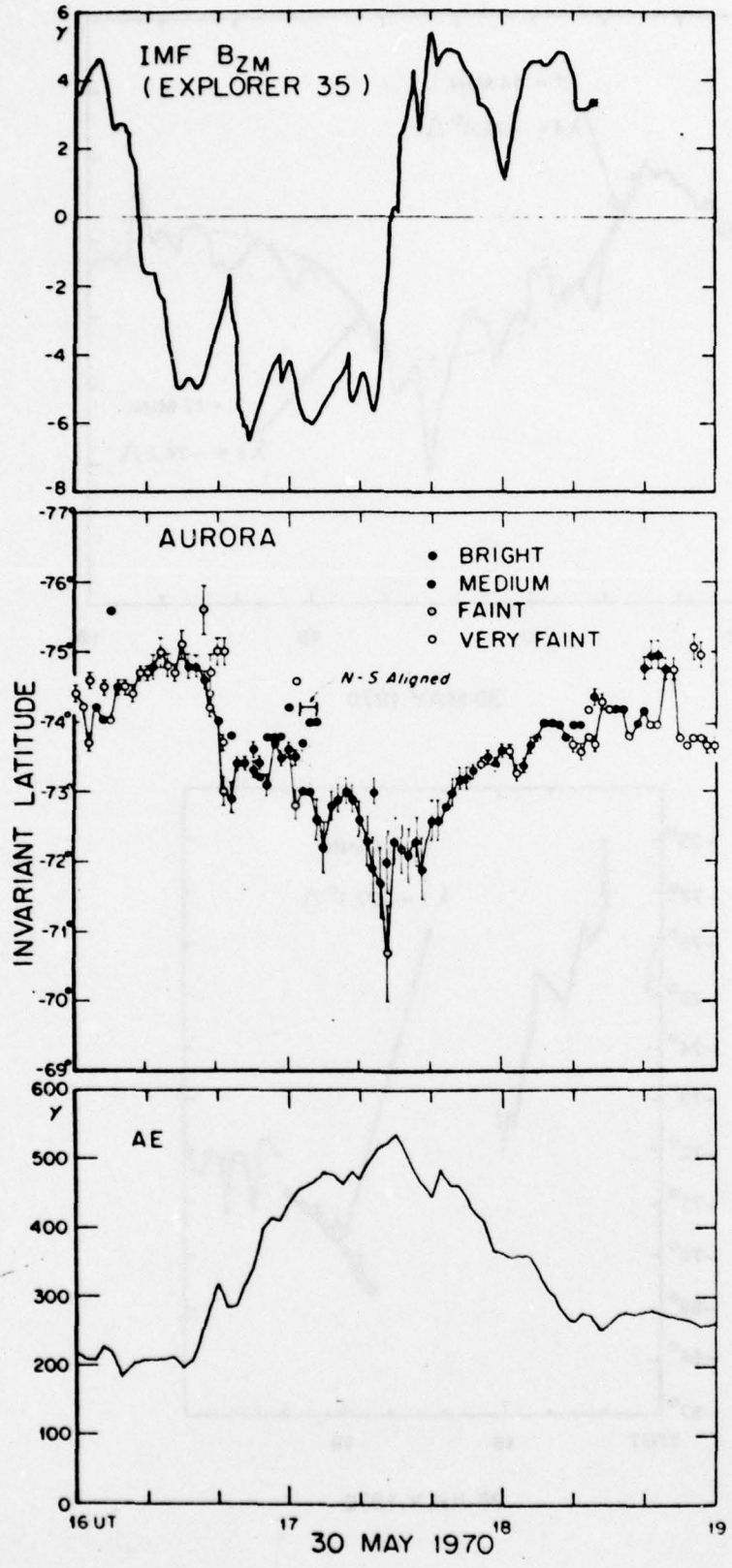
IMF $B_{ZM}$
(EXPLORER 35)
γ
6
4
2
0
-2
-4
-6
-8
AURORA
BRIGHT
MEDIUM
FAINT
VERY FAINT
N-S Aligned
INVARIANT LATITUDE
-77°
-76°
-75°
-74°
-73°
-72°
-71°
-70°
-69°
AE
γ
600
500
400
300
200
100
0
16 UT
17
18
19
30 MAY 1970

FIGURE 8

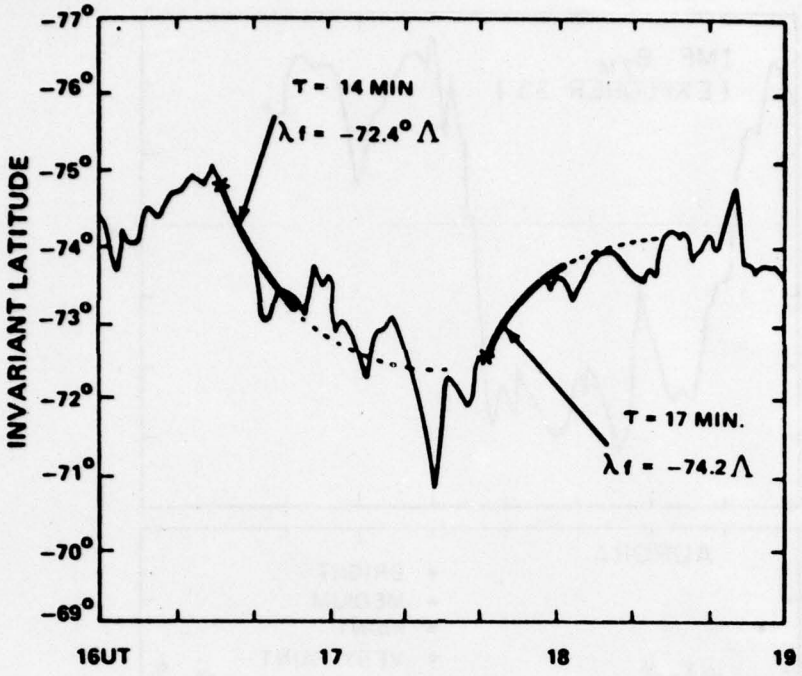
INVARIANT LATITUDE
-77°
-76°
-75°
-74°
-73°
-72°
-71°
-70°
-69°
τ = 14 MIN
λf = -72.4° Λ
τ = 17 MIN.
λf = -74.2 Λ
16UT
17
18
19
30 MAY 1970

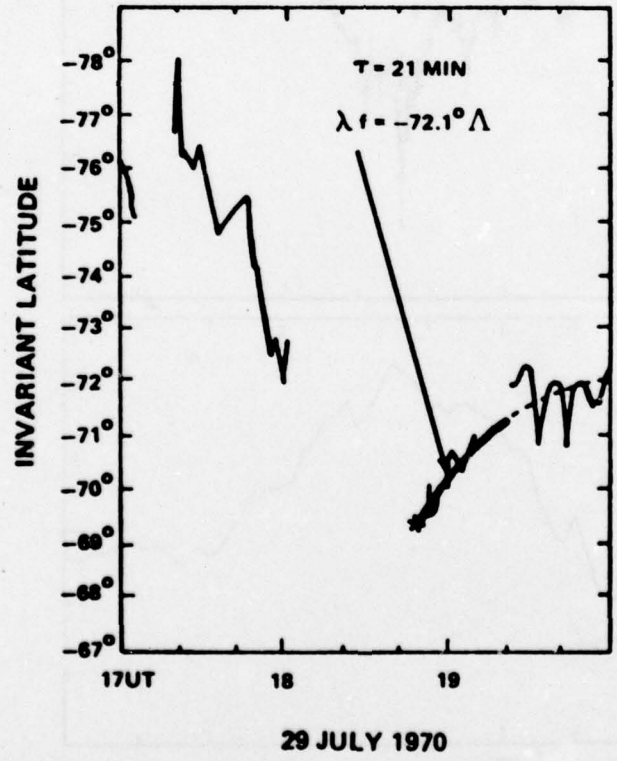
INVARIANT LATITUDE
-78°
-77°
-76°
-75°
-74°
-73°
-72°
-71°
-70°
-69°
-68°
-67°
τ = 21 MIN
λf = -72.1° Λ
17UT
18
19
29 JULY 1970

FIGURE 9

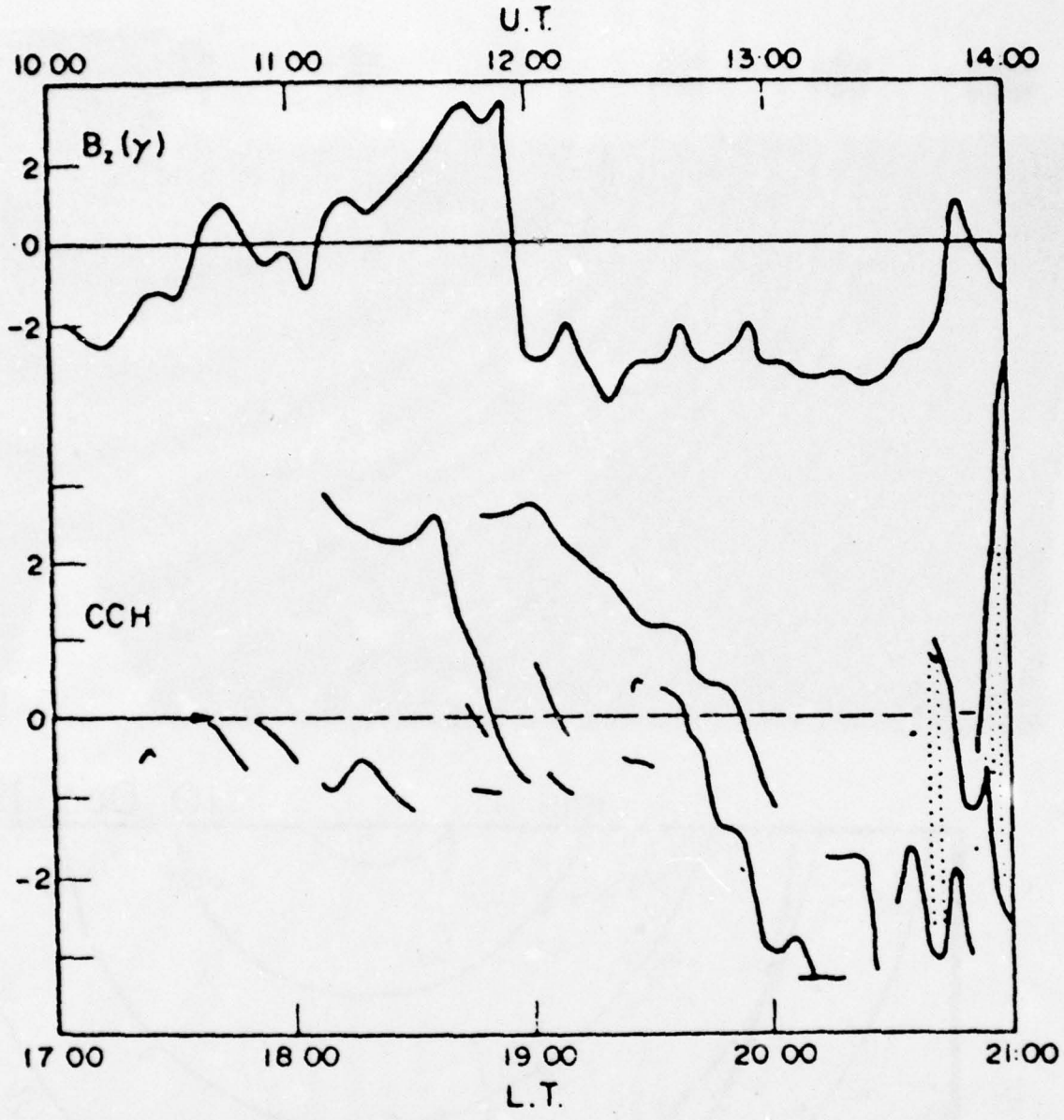
U.T.
10 00
11 00
12 00
13 00
14.00
$B_z(\gamma)$
2
0
-2
2
CCH
0
-2
17 00
18 00
19 00
20 00
21:00
L.T.

FIGURE 10

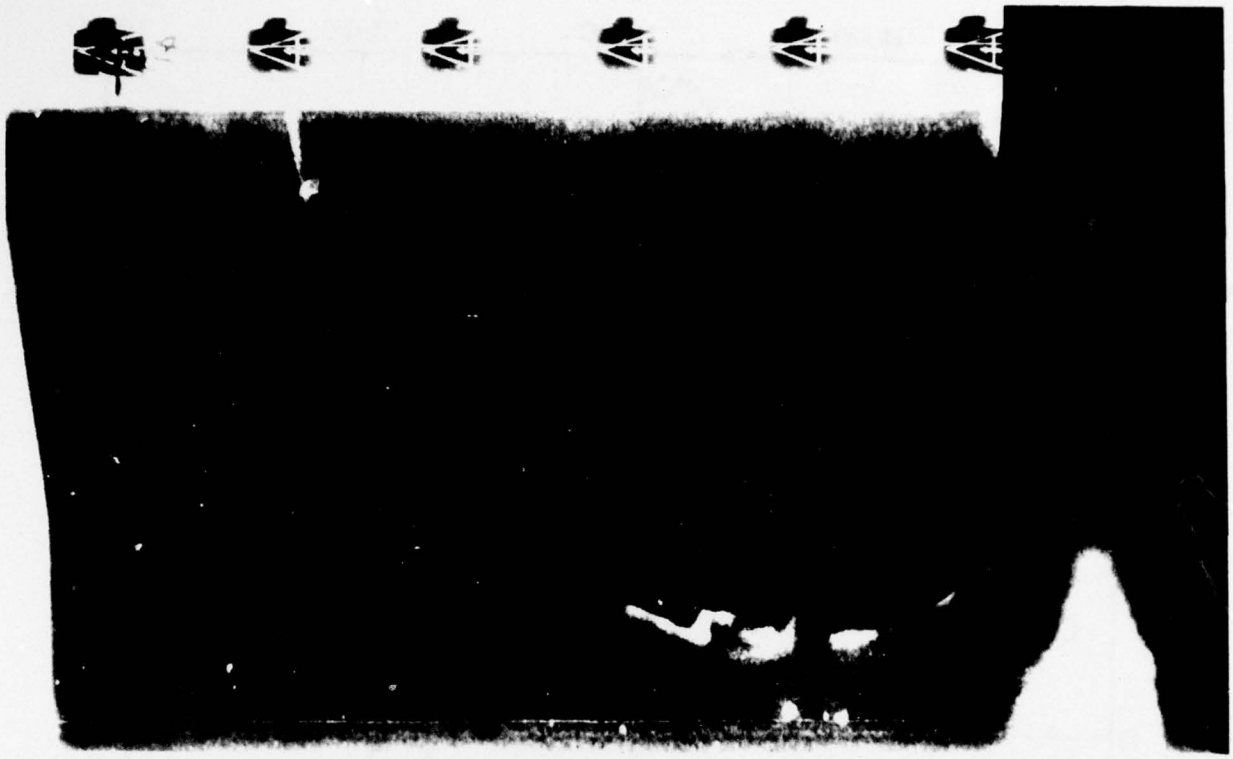

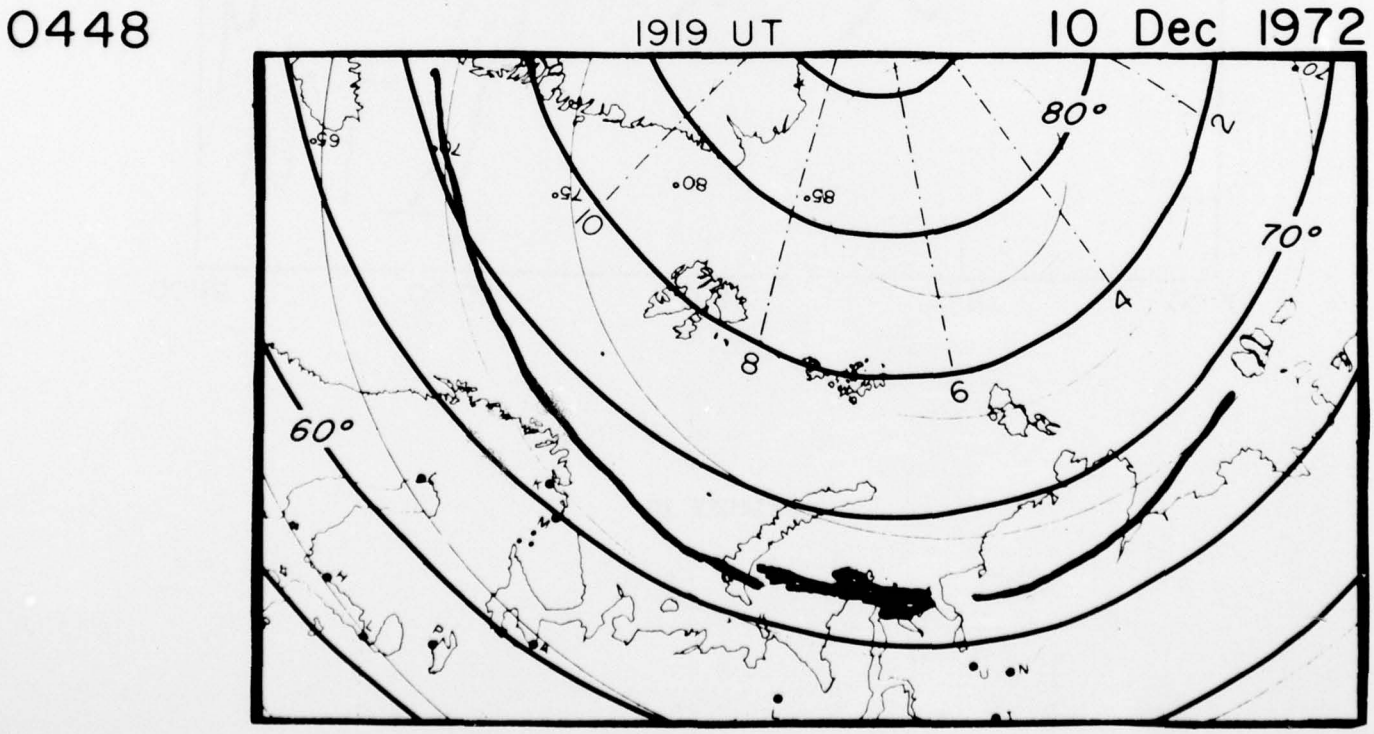


FIGURE 11

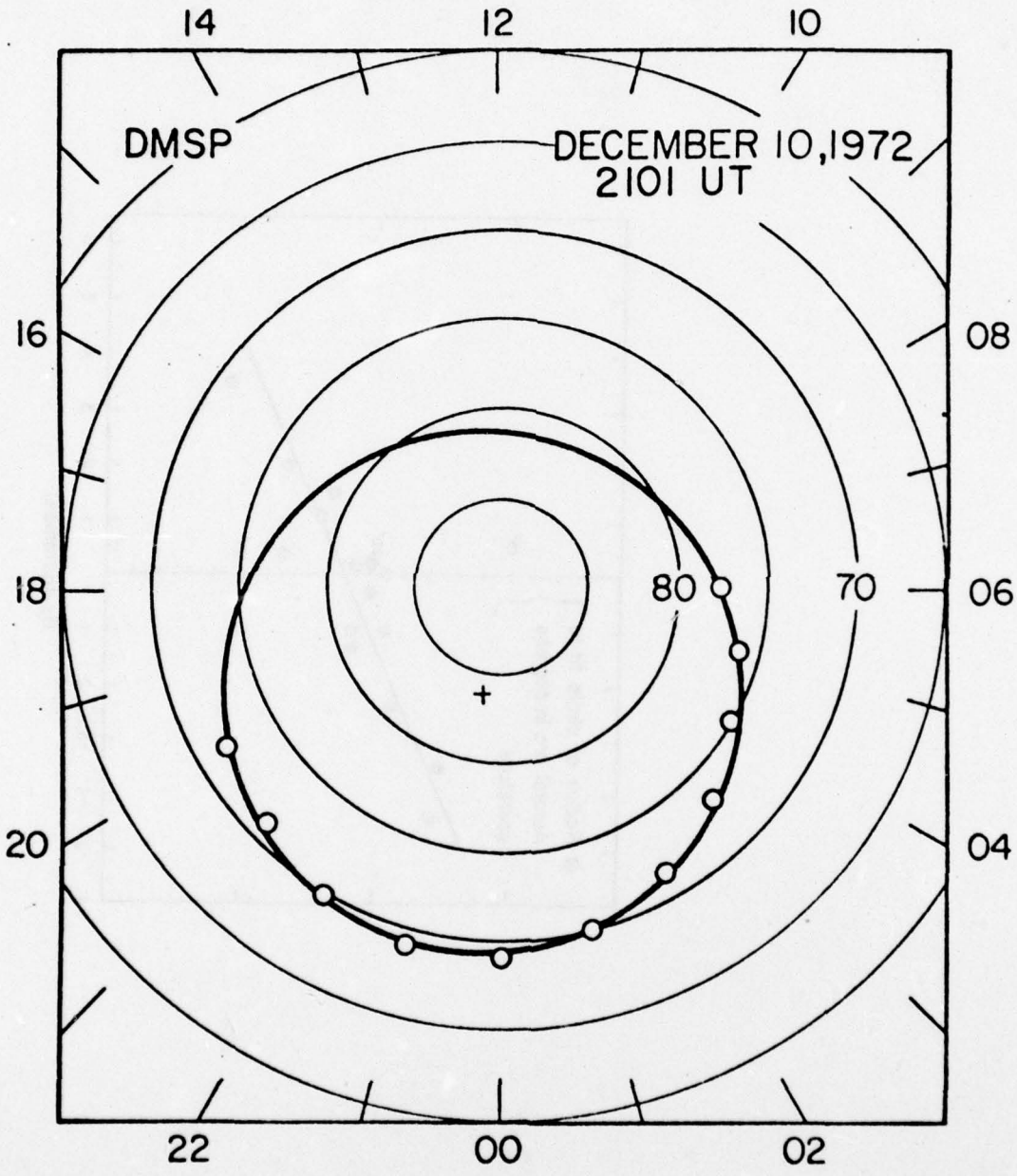
14
12
10
DMSP
DECEMBER 10,1972
2101 UT
16
08
18
80
70
06
20
04
22
00
02

FIGURE 12

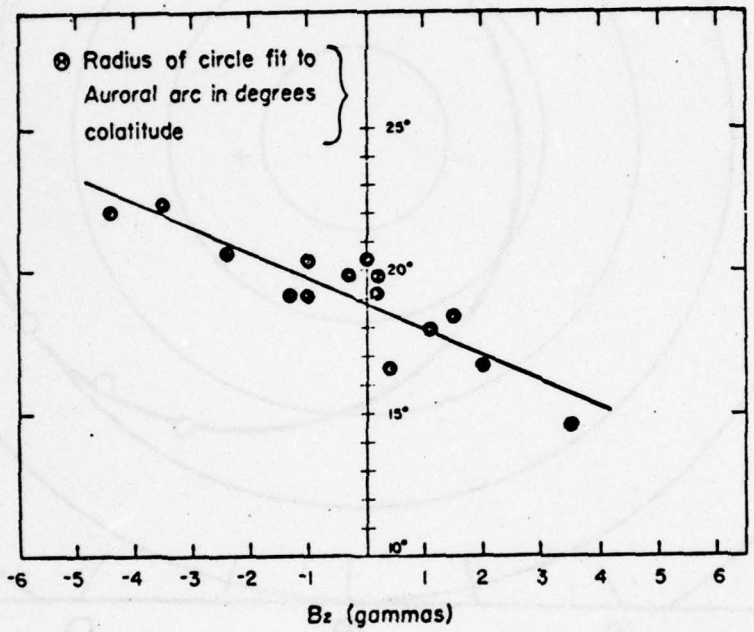
⊗ Radius of circle fit to Auroral arc in degrees colatitude
25°
20°
15°
10°
-6 -5 -4 -3 -2 -1 1 2 3 4 5 6
Bz (gammas)

FIGURE 13

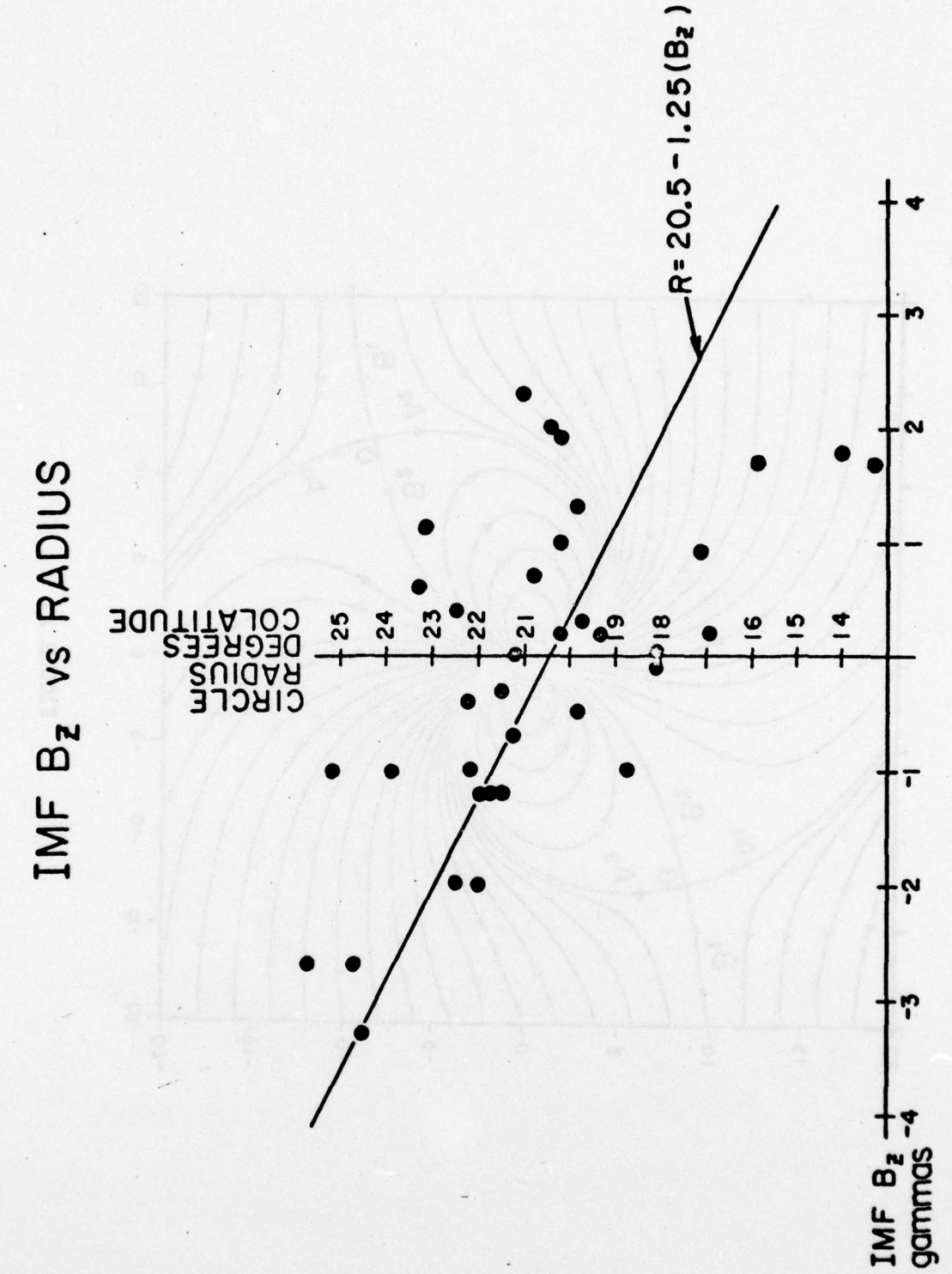
IMF $B_z$ vs RADIUS
CIRCLE RADIUS DEGREES COLATITUDE
25
24
23
22
21
19
18
16
15
14
R= 20.5 - 1.25($B_z$)
IMF $B_z$ gammas
4
3
2
1
-1
-2
-3
-4

FIGURE 14

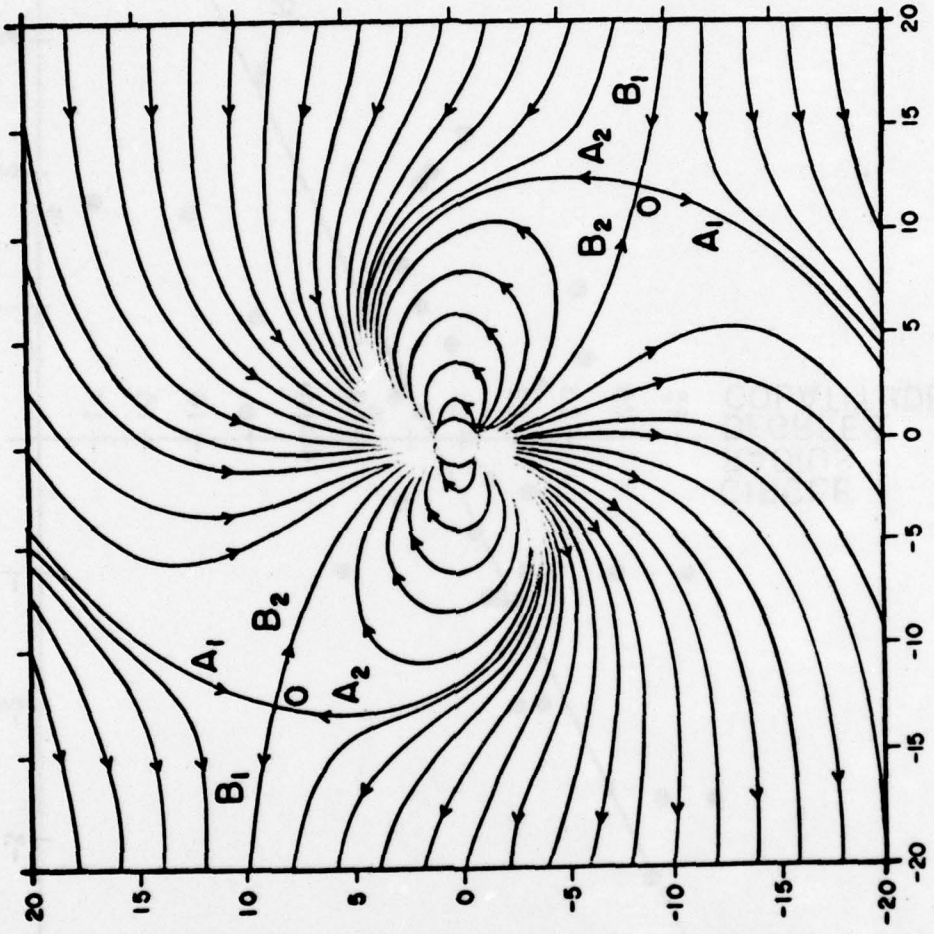


FIGURE 15

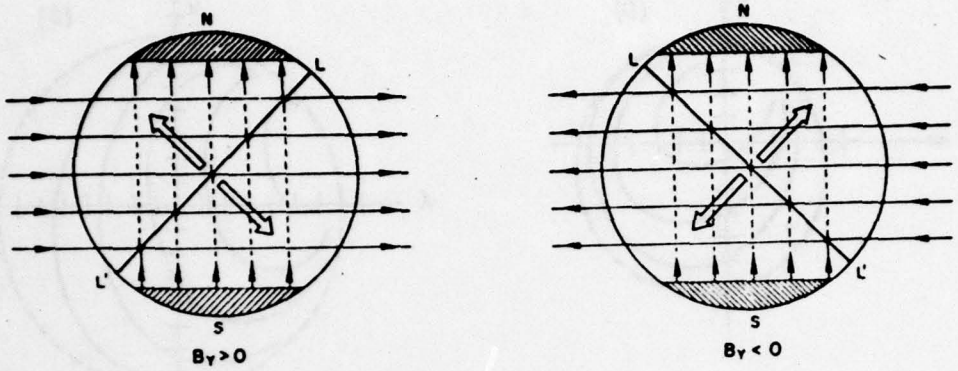


FIGURE 16

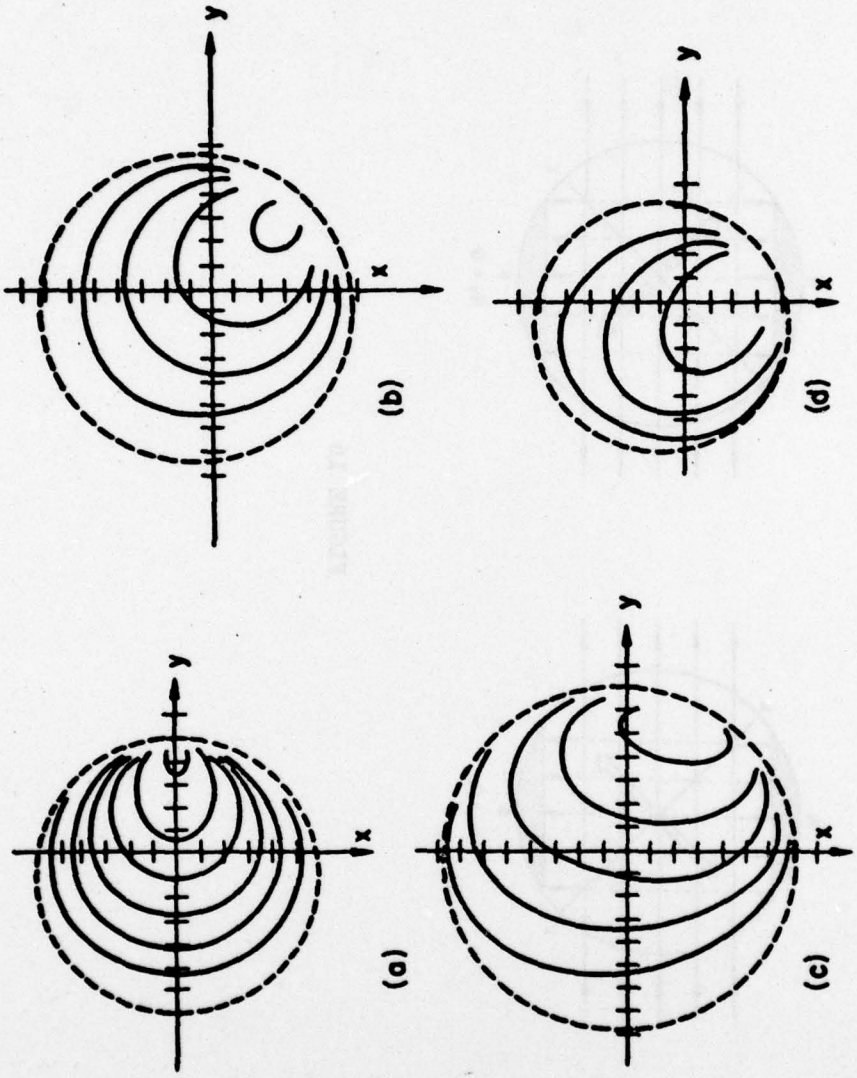


FIGURE 17

## IMF $B_Y$ vs Y COOR. OF CENTER (ONLY)

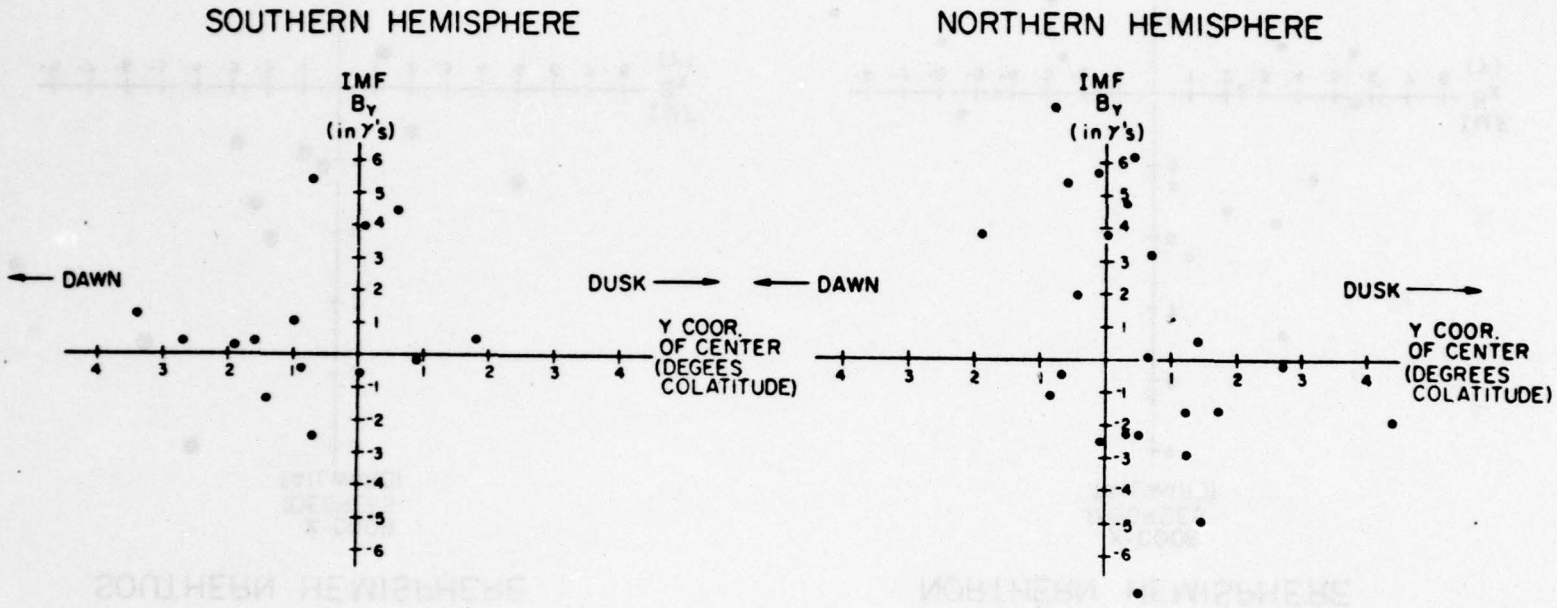


FIGURE 18

# IMF $B_X$ vs X COOR. OF CENTER(ONLY)

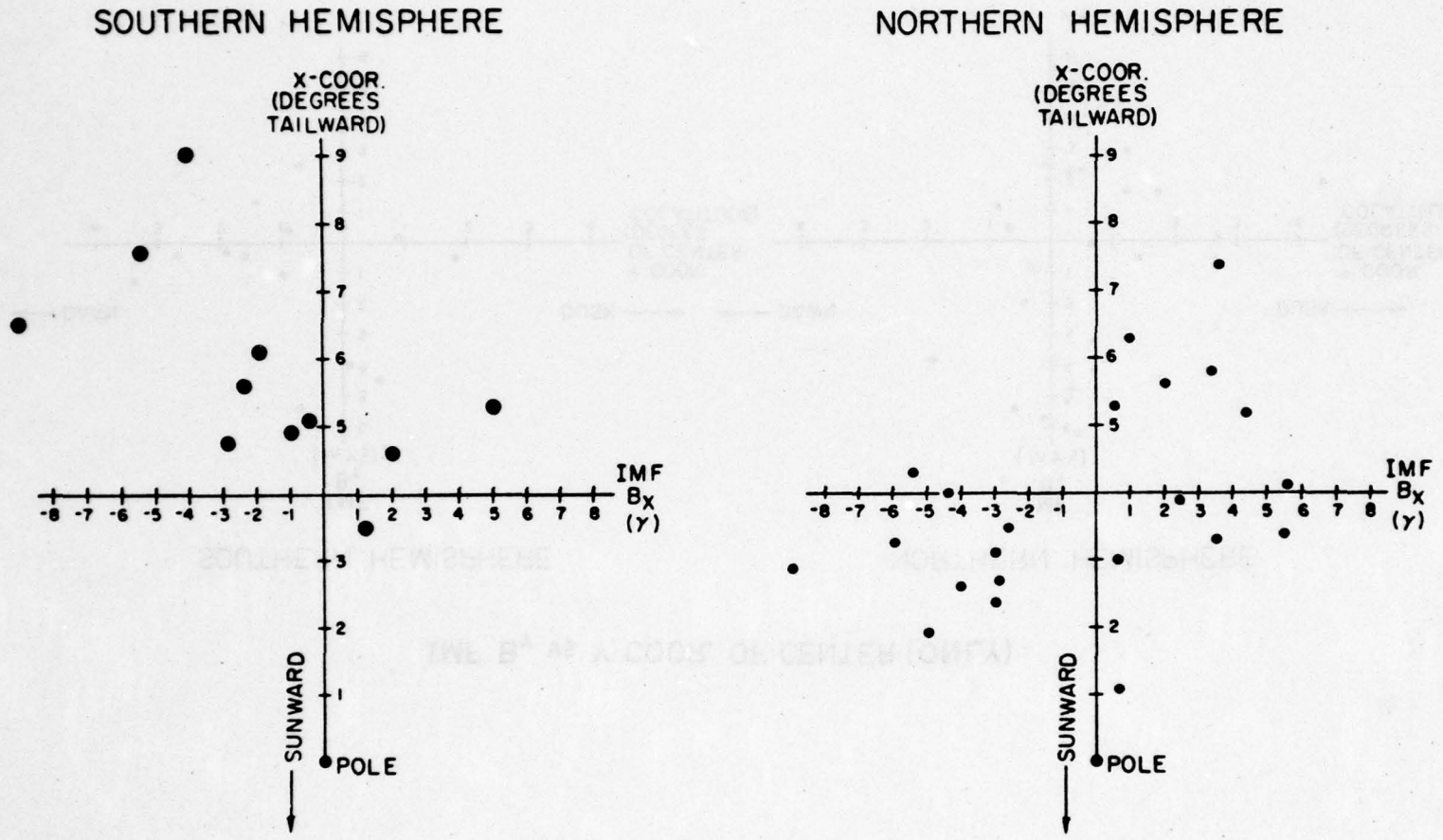


FIGURE 19

## PUBLICATIONS

1. Auroral Circle - Delineating the Poleward Boundary of the Quiet Auroral Belt, by C.-I. Meng, R. H. Holzworth and S.-I. Akasofu, *J. Geophys. Res.*, *82*, 164, 1977.
2. Intense Uniform Precipitation of Low-Energy Electrons Over the Polar Cap, by C.-I. Meng and H. W. Kroehl, *J. Geophys. Res.*, *82*, 2305, 1977.
3. Dawn-Dusk Gradient of the Low-Energy Electrons Over the Polar Cap and Its Relation to the Interplanetary Magnetic Field, by C.-I. Meng, S.-I. Akasofu, and K. A. Anderson, *J. Geophys. Res.*, *82*, 5271, 1977.
4. Observations of Auroral Westward Traveling Surges and Electron Precipitations, by C.-I. Meng, A. L. Snyder, Jr. and H. W. Kroehl, *J. Geophys. Res.*, *83*, 575, 1978.
5. Electron Precipitations and Polar Auroras, by C.-I. Meng, *Space Science Reviews*, (in press), 1978.
6. Electron Precipitation of Evening Diffuse Aurora and Its Conjugate Electron Fluxes Near the Magnetospheric Equator, by C.-I. Meng, B. Mauk, and C. E. McIlwain, *J. Geophys. Res.*, (in press), 1979.
7. Conjugate Low Energy Electron Observations Made by ATS-6 and DMSP-32 Satellites, by C.-I. Meng, *Geophysical Monograph Series, Vol. 21*, (in press), 1979.
8. Polar Cap Variations and the Interplanetary Magnetic Field, by C.-I. Meng, *Space Science Reviews*, (in press), 1979.

This list speaks for the effort which we put into this project as well as the quantity and quality of the results produced under this contract. Reprints or preprints are available to interested parties by contacting the following addressee:

Dr. Ching -I. Meng
Space Physics and Instrumentation Group
Applied Physics Laboratory
Johns Hopkins University
Laurel, Maryland 20810
Telephone: (301) 953-7100 ext. 682

Among these results, a paper on the auroral circle published in the January 1977 issue of the Journal of Geophysical Research was selected as the feature topic in Space Sciences by The Science News in their February 1977 issue under the title Earth's Auroral Tiara. The news clipping of this article is attached.

From *Science News, Vol. III,* p. 106, February, 1977.

# SPACE SCIENCES

## Earth's auroral tiara

The earth's crown of light, the band of glowing auroras that bedecks the Northern Hemisphere, seems more elegant still with a research team's calculation that the poleward edge of the band, rather than being random or distorted, forms a near-perfect circle.

It is not centered around the geographic north pole, nor even around the geomagnetic pole. More than 50 satellite photos showing auroral arcs along portions of the band's edge, however, seem to fit in a pattern that is nonetheless compellingly round. The photos, taken as part of the U.S. Air Force's Defense Meteorological Satellite Program, have been analyzed by Ching Meng and Robert H. Holzworth of the University of California at Berkeley and Syun Akasofu of the University of Alaska in Fairbanks.

Prior studies by others, based on earth-based and aircraft photography, had suggested other auroral distributions such as an oval, displaced about 3° along the midnight meridian from the dipole axis, or a pair of horseshoes, one on the day side and a larger one on the right side, according to the authors. However, they report in the Jan. 1 JOURNAL OF GEOPHYSICAL RESEARCH, the satellite photos have provided "the first opportunity to study the instantaneous distribution of auroras over a large portion of the polar regions."

Although the photos do not show the full 360° of the belt, a mathematical curve-fitting technique reported two years ago by Holzworth and Meng has been used to fit the partial arcs to closed loops. Three different statistical analyses indicate that a circle is a good fit, or at least that the ratio between major and minor axes is a nearly round $0.995 \pm 0.004$. The centers of the auroral circles implied by the arcs in the photos seem to be concentrated in a circular area about 6° across, centered about 4.2° away from the geomagnetic pole in the direction of a meridian defined as 0015 "dipole-magnetic local time." The radii of the circles fall in the range of about $19° \pm 5°$.